VOLUME 102 | SUPPLEMENT 1 | MARCH 2022

LI

LABORATORY INVESTIGATION

THE BASIC AND TRANSLATIONAL PATHOLOGY RESEARCH JOURNAL

ABSTRACTS (1111–1144)

PANCREAS, GALLBLADDER, AMPULLA, AND EXTRA-HEPATIC BILIARY TREE

2022

USCAP 111TH ANNUAL MEETING

REAL INTELLIGENCE

MARCH 19–24, 2022 LOS ANGELES, CALIFORNIA

Published by SPRINGER NATURE
www.ModernPathology.org

USCAP Creating a Better Pathologist
AN OFFICIAL JOURNAL OF THE UNITED STATES AND CANADIAN ACADEMY OF PATHOLOGY

EDUCATION COMMITTEE

Rhonda K. Yantiss
Chair

Kristin C. Jensen
Chair, CME Subcommittee

Laura C. Collins
Chair, Interactive Microscopy Subcommittee

Yuri Fedoriw
Short Course Coordinator

Ilan Weinreb
Chair, Subcommittee for Unique Live Course Offerings

Carla L. Ellis
Chair, DEI Subcommittee

Adebowale J. Adeniran
Kimberly H. Allison
Sarah M. Dry
William C. Faquin
Karen J. Fritchie
Jennifer B. Gordetsky
Levon Katsakhyan, Pathologist-in-Training
Melinda J. Lerwill
M. Beatriz S. Lopes
Julia R. Naso, Pathologist-in-Training
Liron Pantanowitz
Carlos Parra-Herran
Rajiv M. Patel
Charles "Matt" Quick
David F. Schaeffer
Lynette M. Sholl
Olga K. Weinberg
Maria Westerhoff

ABSTRACT REVIEW BOARD

Benjamin Adam
Oyedele Adeyi
Mariam Priya Alexander
Daniela Allende
Catalina Amador
Vijayalakshmi Ananthanarayanan
Tatjana Antic
Manju Aron
Roberto Barrios
Gregory R. Bean
Govind Bhagat
Luis Zabala Blanco
Michael Bonert
Alain C. Borczuk
Tamar C. Brandler
Eric Jason Burks
Kelly J. Butnor
Sarah M. Calkins
Weibiao Cao
Wenqing (Wendy) Cao
Barbara Ann Centeno
Joanna SY Chan
Kung-Chao Chang
Hao Chen
Wei Chen
Yunn-Yi Chen
Sarah Chiang
Soo-Jin Cho
Shefali Chopra
Nicole A. Cipriani
Cecilia Clement
Claudiu Cotta
Jennifer A. Cotter
Sonika M. Dahiya
Elizabeth G. Demicco
Katie Dennis
Jasreman Dhillon
Anand S. Dighe
Bojana Djordjevic
Michelle R. Downes
Charles G. Eberhart
Andrew G. Evans
Fang Fan
Julie C. Fanburg-Smith
Gelareh Farshid
Michael Feely
Susan A. Fineberg
Dennis J. Firchau
Gregory A. Fishbein
Agnes B. Fogo
Andrew L. Folpe
Danielle Fortuna
Billie Fyfe-Kirschner
Zeina Ghorab
Giovanna A. Giannico
Anthony J. Gill
Tamar A. Giorgadze
Alessio Giubellino
Carolyn Glass
Carmen R. Gomez-Fernandez
Shunyou Gong
Purva Gopal
Abha Goyal
Christopher C. Griffith
Ian S. Hagemann
Gillian Leigh Hale
Suntrea TG Hammer
Malini Harigopal
Kammi J. Henriksen
Jonas J. Heymann
Carlo Vincent Hojilla
Aaron R. Huber
Jabed Iqbal
Shilpa Jain
Vickie Y. Jo
Ivy John
Dan Jones
Ridas Juskevicius
Meghan E. Kapp
Nora Katabi
Francesca Khani
Joseph D. Khoury
Benjamin Kipp
Veronica E. Klepeis
Christian A. Kunder
Stefano La Rosa
Stephen M. Lagana
Keith K. Lai
Goo Lee
Michael Lee
Vasiliki Leventaki
Madelyn Lew
Faqian Li
Ying Li
Chieh-Yu Lin
Mikhail Lisovsky
Lesley C. Lomo
Fang-I Lu
aDeqin Ma
Varsha Manucha
Rachel Angelica Mariani
Brock Aaron Martin
David S. McClintock
Anne M. Mills
Richard N. Mitchell
Hiroshi Miyamoto
Kristen E. Muller
Priya Nagarajan
Navneet Narula
Michiya Nishino
Maura O'Neil
Scott Roland Owens
Burcin Pehlivanoglu
Deniz Peker Barclift
Avani Anil Pendse
Andre Pinto
Susan Prendeville
Carlos N. Prieto Granada
Peter Pytel
Stephen S. Raab
Emilian V. Racila
Stanley J. Radio
Santiago Ramon Y Cajal
Kaaren K Reichard
Jordan P. Reynolds
Lisa M. Rooper
Andrew Eric Rosenberg
Ozlen Saglam
Ankur R. Sangoi
Kurt B. Schaberg
Qiuying (Judy) Shi
Wonwoo Shon
Pratibha S. Shukla
Gabriel Sica
Alexa Siddon
Anthony Sisk
Kalliopi P. Siziopikou
Stephanie Lynn Skala
Maxwell L. Smith
Isaac H. Solomon
Wei Song
Simona Stolnicu
Adrian Suarez
Paul E. Swanson
Benjamin Jack Swanson
Sara Szabo
Gary H. Tozbikian
Gulisa Turashvili
Andrew T. Turk
Efsevia Vakiani
Paul VanderLaan
Hanlin L. Wang
Stephen C. Ward
Kevin M. Waters
Jaclyn C. Watkins
Shi Wei
Hannah Y. Wen
Kwun Wah Wen
Kristy Wolniak
Deyin Xing
Ya Xu
Shaofeng N. Yan
Zhaohai Yang
Yunshin Albert Yeh
Huina Zhang
Xuchen Zhang
Bihong Zhao
Lei Zhao

To cite abstracts in this publication, please use the following format: **Author A, Author B, Author C, et al. Abstract title (abs#). In "File Title."** ***Laboratory Investigation*** **2022; 102 (suppl 1): page#**

1111 Standardization of Pathologic Sampling and Evaluation of Gallbladder Specimens: Recommendations of the International Study Group on Gallbladder Cancer (ISG-GBC) of International Hepato-Pancreato-Biliary Association (IHPBA)

N. Volkan Adsay[1], Olca Basturk[2], Juan Carlos Roa[3], Bahar Memis[4], Burcin Pehlivanoglu[5], Keetaek Jang[6], Juan Araya[7], Jin-Young Jang[8], Kyoungbun Lee[9], Michelle Reid[10], Prasenjit Das[11], Jill Koshiol[12], Anita Balakrishnan[13], Jagannath Palepu[14], Shailesh Shrikhande[15], Bhawna Sirohi[16], Javier Lendoire[17], Xabier de Aretxabala[18], Itaru Endo[19], Hector Losada[7], Philip de Reuver[20], Shishir Maithel[21], William Jarnagin[2]

[1]Koç University Hospital, Istanbul, Turkey, [2]Memorial Sloan Kettering Cancer Center, New York, NY, [3]Pontificia Universidad Católica de Chile, Santiago, Chile, [4]SBU Sisli Hamidiye Etfal Training and Research Hospital, Istanbul, Turkey, [5]Dokuz Eylul University, Izmir, Turkey, [6]Samsung Medical Center, Seoul, South Korea, [7]Universidad de La Frontera, Temuco, Chile, [8]Seoul National University Hospital, Seoul, South Korea, [9]Seoul National University Hospital, South Korea, [10]Emory University Hospital, Atlanta, GA, [11]All India Institute of Medical Sciences, New Delhi, India, [12]National Cancer Institute, Rockville, MD, [13]Cambridge University Hospitals NHS Trust, Cambridge, United Kingdom, [14]Lilavati Hospital and Research Centre, Mumbai, India, [15]Tata Memorial Hospital, Mumbai, India, [16]Apollo Proton Cancer Centre in Chennai, Chennai, India, [17]Hospital Argerich, Buenos Aires, Argentina, [18]Clinica Alemana, Santiago, Chile, [19]Yokohama City University, Yokohama, Japan, [20]Radboud University Medical Center, Nijmegen, Netherlands, [21]Emory University, Atlanta, GA

Disclosures: N. Volkan Adsay: None; Olca Basturk: None; Juan Carlos Roa: None; Bahar Memis: None; Burcin Pehlivanoglu: None; Keetaek Jang: None; Juan Araya: None; Jin-Young Jang: None; Kyoungbun Lee: None; Michelle Reid: None; Prasenjit Das: None; Jill Koshiol: None; Anita Balakrishnan: None; Jagannath Palepu: None; Shailesh Shrikhande: None; Bhawna Sirohi: None; Javier Lendoire: None; Xabier de Aretxabala: None; Itaru Endo: None; Hector Losada: None; Philip de Reuver: None; Shishir Maithel: None; William Jarnagin: None

Background: ISG-GBC of IHPBA has identified pathologic standardization as the top priority before clinical trials can be initiated.

Design: 7 international consensus meetings were held and the literature was analyzed. A standard and practical grossing and sampling protocol was designed.

Results: Recommendations: I. If no clinical/gross cancer: 1. No history/findings: Considering > 50% GBC are clinically/grossly-unapparent, all GBs ought to be examined in minimum 1 block including 1 en-face section of cystic duct margin (to serve as shaved margin if a cancer is found) and a transmural slice extending from fundus to neck per the Chilean/Roa protocol. 2. Risk history. Patients with reflux cholecystopathy, PBM and PSC warrant careful examination (4 blocks). 3. After microscopy of routine section. A. “Low risk” mucosal changes (atypia, intestinal and foveolar metaplasia,) 3 additional blocks to rule out CIS. B. If true dysplasia/carcinoma, specimen is re-grossed, surfaces inked, and submitted. Mapping is not necessary but valuable. II. Gross findings of risk. Hyalinizing cholecystitis is sampled extensively, and polyps and adenomyomas, entirely. If intracholecystic neoplasm, the uninvolved mucosa must also be sampled substantially (≥ 5 blocks). III. Approach to carcinoma detected microscopically. 1.A case must not be classified as Tis/T1 (“early GBC”) unless the GB is submitted entirely to carefully exclude T2, preferably in consultation with experts. An attempt should be made to further subclassify early GBCs per Santiago consensus criteria. 2. A case must not be classified as T2 unless GB is examined extensively to rule out T3 with at least 4 blocks of the tumor-to-surfaces, but preferably by entire submission. 3. For T2s, it is advised that the depth of invasion from the lower edge of the muscularis is documented along with a notation of whether it is superficial/minimal (< 1mm into the perimuscular tissue, and confined to fiber-rich layer, and is > 1mm from external surfaces), versus deeper. T2 within 1 mm of external surfaces often behave like T3. IV. Overt/gross GBC with deep infiltration: 5 tumor sections and ≥ 4 of the closest surfaces; for T2 and lesser, revert to protocols above. In all cases, the location (hepatic vs serosal) and LNs to be documented per AJCC.

Conclusions: These recommendations will ensure proper characterization of pathology, standardized documentation for comparability in the literature, as well as for determination of eligibility in clinical trials.

1112 The Importance of Lymph Node Drainage Areas of Ampullary Carcinomas

Kadriye Akar[1], Emine Bozkurtlar[1], Pelin Bagci[1], Serdar Balci[2]
[1]Marmara University, Istanbul, Turkey, [2]Independent Consultant, Turkey

Disclosures: Kadriye Akar: None; Emine Bozkurtlar: None; Pelin Bagci: None; Serdar Balci: None

Background: Locations of metastatic lymph nodes of ampullary carcinomas are not being reported according to the current CAP Cancer Protocole Templates. But the lymphatic drainage patterns might have a prognostic implication.

Design: 102 consequent ampullary carcinomas were retrieved from the institutional archives all of which sampled with the same method (Adsay or bivalving method, and orange peeling for the lymph nodes), and tumor was totally sampled in every case as well. Orange peeled lymph nodes were already defined and reported in specific groups in their original reports (Table).

Results: Female/Male was 43/59. Mean age was 65 (39-84). Mean diameter was 2.3 cm. IAPN associated cases were 38.4%, ductal type was 49.5%, periampullary cases were 7.1%, and NOS type cases were 5.1% of the cohort. Lymphatic invasion was seen in 86.1%, and vascular invasion was seen in 62.4% cases. 47.5% cases were in early stages (Tis+T1+T2), and 52.5% cases were in advanced stages (T3). Lymph node metastasis was found in 69.6% of the cases (N1: 37%, N2: 32.6%). Lymph node draining patterns are shown in the Table. Multivariable survival analysis was done to see whether these drainage areas have an effect over survival. When there was metastasis in the anterior group lymph nodes the median survival was 39.1 [17.2 - NA, 95% CI] months (HR: 0.54 (0.26-1.12, p=0.097). When there was metastasis in the posterior group lymph nodes the median survival was 51.1 [27.9 - NA, 95% CI] months (HR: 0.83 (0.44-1.55, p=0.554) .

METASTATIC LYMPH NODES	N	%
Anterior Group	34	33.3
Anterior Pancreas	9	8.8
	16	15.6
Anterior Pancreatoduodenal	9	8.8
Inferior Head		
Posterior Group	87	85.2
Posterior Pancreas	37	36.2
	43	42.1
Posterior Pancreatoduodenal	0	0
Superior Head	7	6.8
Common bile Duct		
Curvature Group	4	3.9
Greater Curvature	2	1.9
	2	1.9
Lesser curvature		
Others	9	8.8

Conclusions: Dominant drainage area was shown to be the posterior surface in our cohort. Even though the statistical work up did not show a significant result, presence of a metastatic lymph node in the anterior drainage areas had a slight negative effect over survival compared to a metastatic posterior surface lymph node (median survival months 39,1 and 51.1 respectively). These results also show that these peripancreatic lymph node areas should be separately reported in the synoptics.

1113 Tumor Budding and Poorly Differentiated Clusters are Unfavorable Prognostic Factors in Pancreatic Ductal Adenocarcinoma, as Validated by the ITBCC Scoring System

Sarah Anderson[1], Krutika Patel[2], Wadad Mneimneh[3], Nadia Hameed[4], Marcus Tan[2], Florencia Jalikis[2]
[1]The University of Alabama at Birmingham, Birmingham, AL, [2]Vanderbilt University Medical Center, Nashville, TN, [3]Case Western Reserve University, Cleveland, OH, [4]The University of Texas MD Anderson Cancer Center, Houston, TX

Disclosures: Sarah Anderson: None; Krutika Patel: None; Wadad Mneimneh: None; Nadia Hameed: None; Marcus Tan: None; Florencia Jalikis: None

Background: Pancreatic ductal adenocarcinoma (PDAC) is a highly aggressive malignancy, that escapes early detection and lacks effective therapeutic options. Tumor budding (TB) and poorly differentiated clusters (PDC) are associated with epithelial-mesenchymal transition, and linked to tumor invasion, progression, and drug resistance in colorectal, breast, and gastric carcinomas. The lack of standardized scoring systems has precluded its inclusion in histopathological reporting of PDAC. In this study, we analyzed TB and PDC as markers of prognostication in non-neoadjuvant PDAC.

Design: We analyzed non-neoadjuvant cases of PDAC from our institutional cohort. TB, PDC were independently scored by three trained pathologists on H&E-stained tumor sections, assessing the densest TB and PDC area at the invasive tumor front at 200x magnification (one hotspot,0.785mm^2) as per the ITBCC scoring system (International Tumor Budding Consensus Conference 2016). Scoring groups were low score (0-4 TB), intermediate score (5-9 TB) and high score (>10 TB). Inter-observer agreement was assessed. Findings were corelated to clinical, histopathologic characteristics. Statistical analysis was performed using one-way ANOVA, Mann-Whitney U, Kaplan-Meier survival on GraphPad Prism v8.0.

Results: Low-score TB was observed in 6/25 (24%), intermediate-score TB in 8/25 (32%), and high-score TB was observed in 11/25 (44%) cases. Interobserver agreement for TB scoring category was strong (weighted kappa value=0.851) between the three pathologists. High-score TB correlates with shorter disease-free survival (*P*=0.0033; HR=0.2111; 95% CI [0.0557- 0.7995]) **(Figure 1).** Also, high-score TB in PDACs has significantly more lymph-node metastasis (24% vs. 6.2% in intermediate-score, 3.5% low-score; *P*=0.0023), a lower overall 3-year survival (22.2% vs. 50% intermediate-score, 100% low-score; *P*=0.002), and trends narrowly towards significance for tumor grading/differentiation. TB scores did not corelate to tumor size, lymphovascular invasion, perineural invasion, and surgical margin involvement. PDC scores on a similar semi-quantitative scale demonstrated comparative statistically significant results.

Figure 1 - 1113

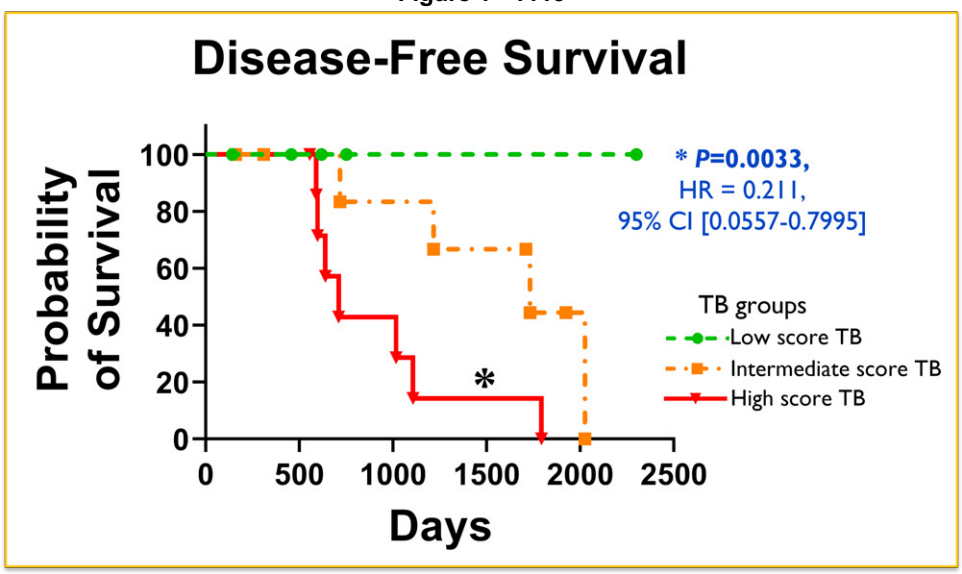

Conclusions: High-score tumor budding is a reproducible unfavorable prognostic factor in pancreatic ductal adenocarcinoma. The incorporation of ITBCC scoring system in standardized histopathological reporting should be facilitated, allowing for better prognostic stratification of pancreatic ductal adenocarcinomas.

1114 Progression of the Immune Response in Matched Intraductal Papillary Mucinous Neoplasms and Associated Invasive Ductal Adenocarcinomas

Naziheh Assarzadegan[1], Braxton Alicia[2], Dwayne Thomas[3], Laura Wood[4], Elizabeth Thompson[4]
[1]University of Michigan, Ann Arbor, MI, [2]Johns Hopkins Medicine, Baltimore, MD, [3]Johns Hopkins University, Baltimore, MD, [4]Johns Hopkins Hospital, Baltimore, MD

Disclosures: Naziheh Assarzadegan: None; Braxton Alicia: None; Dwayne Thomas: None; Laura Wood: None; Elizabeth Thompson: None

Background: Little is understood about the evolution of the immune response and tumor immune microenvironment (TME) as neoplasia progresses from non-invasive precursor lesions to invasive malignancies. Intraductal papillary mucinous neoplasms (IPMN) are cystic precursor lesions to invasive pancreatic ductal adenocarcinomas (PDAC). When they co-exist with an associated invasive PDAC these large precursors provide an opportunity to isolate and study the TME of each type of neoplasia separately.

Design: Whole slides from 24 resection specimens with precursor IPMN and matched invasive PDAC were stained for AE1/3, CD45, CD20, CD4, CD8, CD68, FoxP3, LAG3, PD-1, PD-L1, and VISTA. Immunostained slides were scanned at 20x on a Hamamatsu NanoZoomer XR digital slide scanner. Slides were annotated for representative areas of IPMN and associated invasive PDAC using HALO (Indica Labs). The IPMN annotations included an area of stroma 200 µm deep to the basement membrane. Cells expressing each marker were quantified with HALO. Density of cells calculated as cells/mm^2.

Results: IPMNs demonstrated an active TME with infiltration of immunosuppressive and regulatory cells: Foxp3+ and CD68+ and expression of immune checkpoint proteins: LAG3, PD-1, PD-L1 and VISTA. While no overall difference in CD45+ infiltrating cells was seen between IPMN and matched invasive PDAC on average, there was marked modulation of immune cell subsets with progression from precursor lesion to invasion. The density of the following cell subsets increased significantly in PDAC as compared to their matched IPMN: CD68+ cells, $p<0.001$; Foxp3+ cells, $p=0.04$; LAG3+ cells, $p=0.017$ and PD-L1+ cells, $p=0.03$. No significant differences were seen in density of CD20+, CD4+, CD8+, PD-1+ or VISTA+ cells.

Conclusions: The infiltration pattern of IPMNs suggests that groundwork for the immunosuppressive TME in PDAC may begin far prior to the presence of an invasive PDAC. Immune cell subsets evolved as tumors progressed from IPMNs to PDAC in matched patients, with increases seen in immunosuppressive cells and in regulatory immune checkpoint proteins. The presence of immunosuppression in precursor lesions, paired with modulation of the TME as PDAC develops, suggests multiple time points for potential intervention with immune-based therapies, both in a prophylactic and treatment paradigm. Additional studies are crucial to best understand when and how immune-based treatments can be used to alter the TME at different stages of tumor development.

1115 Features of Neoplastic and Non-Neoplastic Biliary Biopsies: Preliminary Findings from a Large Database

Andrea Barbieri[1], Yueming Cao[1], James Garritano[1], Anuj Verma[1], Donghai Wang[1], Ilke Nalbantoglu[1]
[1]Yale School of Medicine, New Haven, CT

Disclosures: Andrea Barbieri: None; Yueming Cao: None; James Garritano: None; Anuj Verma: None; Donghai Wang: None; Ilke Nalbantoglu: None

Background: Neoplasms of the biliary tree are challenging to diagnose due to complex anatomy with difficult access. Intraductal biopsies (bx) are challenging specimens where overdiagnosis may generate unnecessary resections that result in significant patient morbidity. However, inability to make a timely accurate diagnosis (dx)of malignancy may delay treatment. There are no standard guidelines for adequacy or morphologic interpretation of these bx. Further characterization may help inform optimal assessment and timely diagnosis. We studied features of specimen quality and histology in a large patient cohort with neoplastic (NEO) and non-neoplastic/negative (NEG) diagnoses (dx) over a 10-year period.

Design: Biliary bx with a dx of NEO or NEG (2010-2020) were included. Ampullary bxs, needle cores, and metastatic lesions were excluded. Dx were categorized based on final pathology reports and the slides were reviewed blindly (ALB, IN). NEO was defined as cases with a dysplasia or carcinoma. Features recorded included: number and size of fragments, additional re-cuts/stains, percent (%) epithelium (assessed in intact fragments composed of epithelium and stroma), % detached epithelium, presence of necrosis, bacteria/yeast, ulcer, and smooth muscle. Fisher's exact test and univariate logistic regression were utilized for statistical analysis.

Results: A total of 296 patients were included. 177 (59.8%) were men. Average age was 65.5 (range: 21-94). A total of 447 samples were analyzed and 25% (112/447) were NEO (Table 1). NEO dx was associated with (a/w) male sex (p=0.01). A greater number of tissue fragments correlated with a NEO dx (p=4.05E-06), as did size of largest tissue fragment (p=0.03).

NEO samples had more epithelium compared to stroma than NEG (p=5.48E-06). Presence of smooth muscle and % detached epithelium was similar between the two groups. Ulcer and necrosis were more commonly noted in the NEO cases (p=0.001, and p=0.0005, respectively) (Fig 1A & B). Similarly, presence of bacterial/yeast clusters were more a/w a NEO dx (p=0.03) (Fig1C).

	Non-neoplastic (n: 335)	Neoplastic (n: 112)	p value
M:F	111:92	66:27	**0.01**
Age	65.8	69.2	**0.06**
Specimen Quality and Process			
• **Number of fragments**	Average: 3.99 Median: 4	Average: 5.48 Median: 5	**4.05E-06**
• **Size of largest fragment**	Average: 0.243 mm Median: 0.2 mm	Average: 0.288 mm Median: 0.3	**0.03**
• **Size of smallest fragment**	Average: 0.095 mm Median: 0.05	Average 0.089 mm Median 0.05 mm	0.5
• **Additional levels**	Average: 2.534 Median. 3	Average:1.808 Median: 0	**0.006**
• **Any Immunohistochemical (IHC) stains performed?**	19% (65/335)	28% (32/112)	**0.0473**
AE1/AE3 IHC performed	12% (3/277)	27% (24/90)	**0.001**
Histologic Features			
• **% Epithelium (assessed in intact fragments composed of epithelium and stroma)**	Average: 27.3 Median: 20	Average: 40.6 Median: 30	**5.48E-06**
• **% Detached epithelium**	Average:15.2 Median: 5	Average:10.3 Median: 5	0.11
• **Smooth muscle present**	26% (83/311)	19% (17/89)	0.16
• **Ulcer present**	46% (135/291)	66% (59/89)	**0.001**
• **Necrosis present**	0.6 (2/312)	7.8 (7/89)	**0.0005**
• **Bacteria/yeast present**	18% (57/312)	29% (26/89)	**0.03**

Figure 1 - 1115

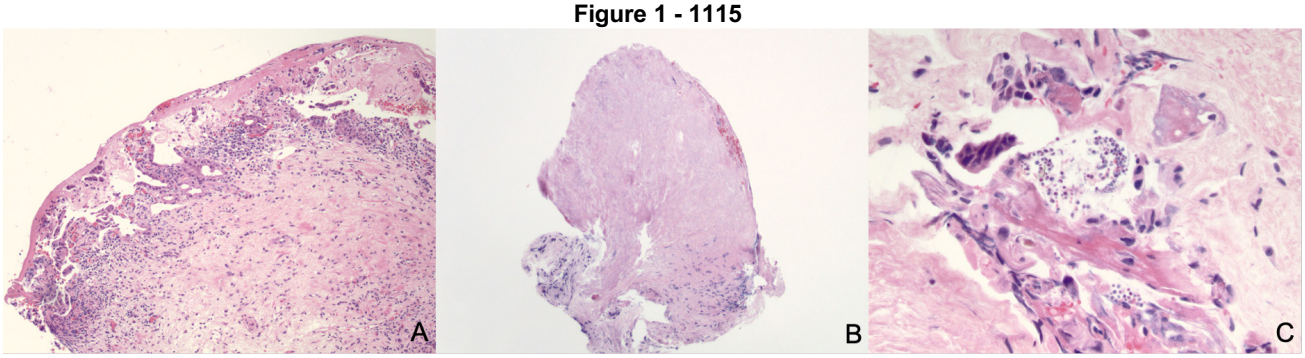

Conclusions: In our cohort, more tissue fragments and larger size of tissue fragments were a/w a NEO dx. Histologically, NEO cases had more epithelium compared to stroma in intact fragments. Presence of ulcer, necrosis, and bacteria/yeast were also a/w a NEO diagnosis. While stent data is not available in this analysis, the features may still help raise suspicion for a neoplastic dx in challenging cases and prompt further work-up or re-bx.

1116 Centrally-Necrotic/Hyalinizing Demarcated (CND) Carcinomas of the Pancreas: A Clinico-Pathologically Distinct Group with Divergent Metaplastic Patterns and High-Grade Characteristics

Duygu Cengiz[1], Burcu Saka[2], Pelin Bagci[3], Emre Altinmakas[4], Emre Bozkurt[1], Ayse Armutlu[5], Burcin Pehlivanoglu[6], Emine Bozkurtlar[3], Michelle Reid[7], Makbule Aydin Mericoz[1], Emrah Alper[1], Jeanette Cheng[8], Claudio Luchini[9], Aldo Scarpa[9], Olca Basturk[10], Gurkan Tellioglu[1], Bengi Gurses[1], N. Volkan Adsay[1]

[1]Koç University Hospital, Istanbul, Turkey, [2]Koç University School of Medicine, Istanbul, Turkey, [3]Marmara University, Istanbul, Turkey, [4]Icahn School of Medicine at Mount Sinai, New York, NY, [5]Koç University, Istanbul, Turkey, [6]Dokuz Eylul University, Izmir, Turkey, [7]Emory University Hospital, Atlanta, GA, [8]Piedmont Atlanta Hospital, Atlanta, GA, [9]University of Verona, Verona, Italy, [10]Memorial Sloan Kettering Cancer Center, New York, NY

Disclosures: Duygu Cengiz: None; Burcu Saka: None; Pelin Bagci: None; Emre Altinmakas: None; Emre Bozkurt: None; Ayse Armutlu: None; Burcin Pehlivanoglu: None; Emine Bozkurtlar: None; Michelle Reid: None; Makbule Aydin Mericoz: None; Emrah Alper: None; Jeanette Cheng: None; Claudio Luchini: None; Aldo Scarpa: None; Olca Basturk: None; Gurkan Tellioglu: None; Bengi Gurses: None; N. Volkan Adsay: None

Background: Pancreatic ductal adenocarcinomas (PDACs) are epitomized by ill-defined schirrous growth of widely scattered glands in desmoplastic stroma.

Design: 25 cases that flouted these defining characteristics and instead formed demarcated centrally necrotic/hyalinizing tumors (akin to those in breast) were analyzed. 7 were identified in re-review of 303 consecutive pancreatectomies; remaining 18, culled from consultations and international collaboration.

Results: Radiology: 26/303 pancreatic tumors revealed central necrosis and demarcation on imaging, most proved to be non-ductal or cystic tumors; 7 proved to be true CND. Pathology: High grade carcinomas with prominent non-glandular patterns and marked intratumoral heterogeneity: Confluent stroma-poor infiltrates/sheets of markedly pleomorphic (monstrous) or multinucleated giant cells with abundant acidophilic/glassy cytoplasm, or rhabdoid cells (INI1 retained in 4/4 tested) focally forming anastomotic pattern, were characteristic. Sheets were often punctuated by mega-mucin vacuoles (mucoepidermoid-like). Dispersed squamoid, pavementing solid clusters were common, but often with minimal/no p40/p63 staining; focal keratinization in only 2. Solid nested pattern with clear cell zones (hypernephroid pattern) was frequent. Stroma-rich infiltration with small solid clusters or cord-like pattern with myxoid matrix was seen as a focal finding in some. Intervening glandular areas occurred in variable amounts, typically also forming back-to-back nodular zones. A peculiar and subtle retrograde-cancerization into lobules was common. Pushing border pattern was also evident in secondary organ invasion (mucosal nodularity, but minimal/no ulcer). None had IPMN/MCN or intraductal growth. Despite demarcation, large tm size (median, 4.6 cm vs 3.6 in PDAC), LN mets (88%), PNI (87%) & LVI (91%) were common. 4 had liver metastasis displaying similar patterns on bx leading to diagnostic challenge. Limited follow up indicated highly aggressive behavior.

Figure 1 - 1116

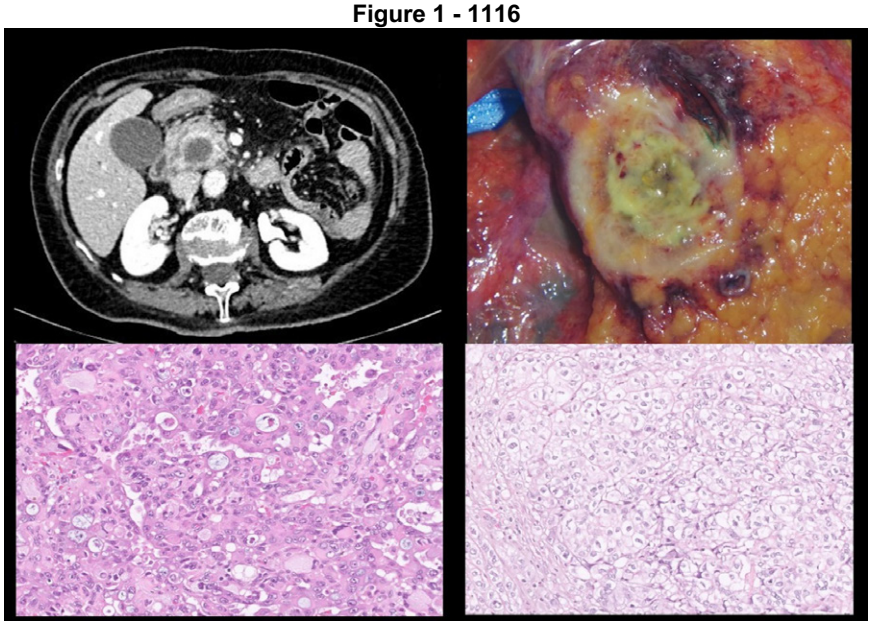

Conclusions: Akin to breast, CND carcinomas also form a distinct group in the pancreas, constitute 3% of all resected tumors, present with the radiologic differential of non-ductal or cystic tumors. Histologically these are high grade carcinomas with compact growth, and various divergent non-glandular (metaplastic) phenotypes, often in combination, that are otherwise highly uncommon in PDACs. Molecular studies are underway to investigate the genotype and possible targetable pathways.

1117 The Topography of Polarizable Collagen Is Significantly Different in Normal Pancreas and Pancreatic Ductal Adenocarcinoma

Mahsa Chitsaz[1], Kevin Eliceiri[2], Bin Lin[2], Adib Keikhosravi[3], Agnes Loeffler[4]
[1]MetroHealth Medical Center, Cleveland, OH, [2]University of Wisconsin-Madison, Madison, WI, [3]Center for Cancer Research, National Cancer Institute, Bethesda, MD, [4]MetroHealth System, Case Western Reserve University, Cleveland, OH

Disclosures: Mahsa Chitsaz: None; Kevin Eliceiri: None; Bin Lin: None; Adib Keikhosravi: None; Agnes Loeffler: None

Background: Changes in collagen alignment in the tumor microenvironment are correlated with tumor growth and progression. Bundled, aligned, and straightened collagen fibers relative to epithelial tumor cells are associated with local invasion and poor survival in studies of pancreatic ductal adenocarcinoma (PDAC). Notably absent in these seminal studies is a description of collagen alignment in normal pancreatic (NP) tissue. We utilize a novel technique, polychromatic polarization microscopy (PPM), to qualitatively evaluate the differences in collagen topography in NP and PDAC. Similar to conventional polarization techniques, PPM is a hardware-based polarization solution that can be added to conventional diagnostic microscopes, but it highlights polarizable fibers at all angles relative to the angle of polarization.

Design: 10 cases each of NP and PDAC were examined with PPM at 1.25x and 20x. The arrangement of polarizable collagen fibers (PCF) in relation to the ductal epithelium and acinar tissue, the spatial arrangement of PCF in relation to each other, and specific characteristics of individual fibers (straightness, polychromasia, thickness, length) were documented.

Results: PCF in NP is arranged in long, delicate, and wavy fibers that lie in orderly bundles perpendicular to the axis of arteries and tubules. At 1.25x, it appears as discontinuous flecks of bright light; at 20x, the corrugation of the fibers can be appreciated as a polychromatic signal in each individual, delicate strand (Table 1). PCF is not attached to epithelial cells except for very short segments that run tangentially to the contour of the duct. In PDAC, PCF is arrayed in long, sweeping fascicles that give a continuous light signal at 1.25x and show loss of polychromasia at 20x. In contrast to the PCF in interlobular septa, PCF in malignant stroma consists of coarse, monochromatic fibers that either course together in long, interwoven fascicles or lie at random angles to one another. PCF may appear attached to malignant epithelium.

Table 1: Comparison of the orientation of polarizable collagen fibers (PCF) in relation to each other and to the epithelium in normal pancreatic tissue and pancreatic ductal adenocarcinoma

	Normal		Pancreatic Ductal Adenocarcinoma	
	Ducts	Lobules	Ducts and Malignant epithelium	Stroma
1.25 X	The speckled pattern of signal in the discrete zone around normal interlobular and intralobular ducts	Long, delicate, monochromatic but slightly wavy fibers in thin septa between acinar lobules No signal within lobules (around acinar cell clusters or islets)	Loss of speckled pattern around interlobular and intralobular ducts	Thick and coarse, monochromatic, oriented in interwoven fascicles
20 X	Periductal stroma gives a polychromatic signal, with periodic alteration in color in individual fibers	Septal PCF is monochromatic and bright, but slightly wavy Short segments of curvilinear signal are sparsely present in association with acinar cells, islets	May be completely absent, or closely associated with epithelium, either in concentrically arranged PCF or attached to the periphery of malignant clusters and extending at angles into the stroma Monochromatic, loss of periodicity	Monochromatic, loss of periodicity Interlacing, long bundles, also individual, monochromatic PCF arranged in random angles to one another (not bundled)
40 X	PCF in periductal stroma oriented in the same axis in relation to one another and perpendicular to the axis of the duct	Sparse PCF signal in relation to acini and islets Individual fibers of PCF in interlobular septa are arranged in orderly bundles in which the fibers are all lying in the same orientation	As at 20x; close association with malignant cells is better appreciated (when present)	As at 20x; better appreciation of loss of periodicity

Figure 1 - 1117

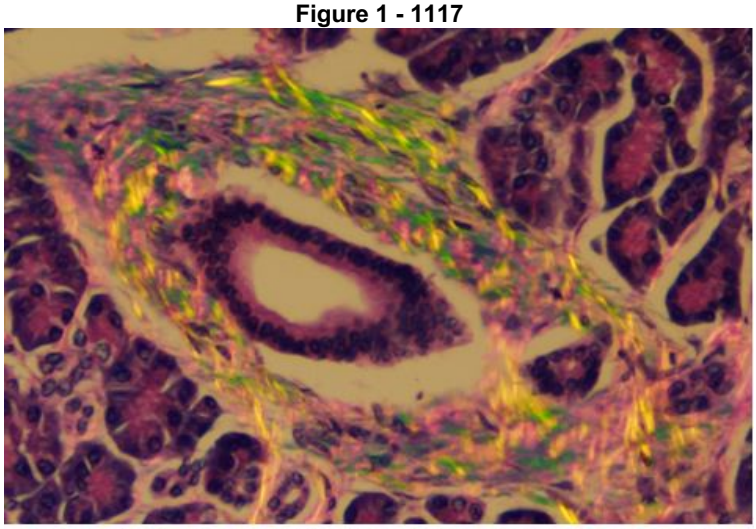

Figure 1. At 20x, Polychromatic light signal around a normal intralobular duct in the pancreas highlights the waviness or corrugation of individual fibers. Differently colored segments are caused by fibers lying at different angles to the polarization filter. The fibers are oriented.

Figure 2 - 1117

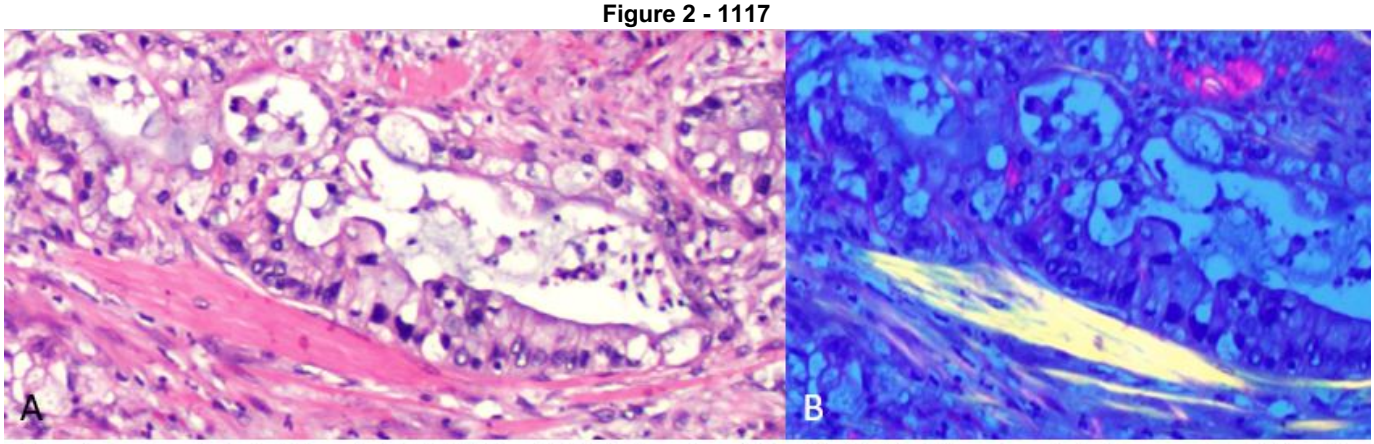

Figure 2. A malignant gland at 40x under bright field (A) and PPM (B). There is no PCF on the left side of the malignant gland, however, the thick bundle of right side is gives very bright, monochromatic light. The fibers are straight, coarse, and bundled. This pattern of PCF is not seen in normal pancreas.

Conclusions: PPM illustrates consistent differences in the arrangement of PCF in benign and malignant pancreatic tissue. While prior studies have described the arrangement of PCF in pancreatic adenocarcinoma as “random” or “disorganized,” PPM demonstrates that the topography of PCF in NP and PDAC is recurrent and consistent. Future studies utilizing PPM will examine the arrangement of PCF in atrophic pancreatic tissue in comparison to PDAC.

1118 Biopsy Evaluation of Pancreatic Neuroendocrine Tumors: Challenges in Interpretation and Correlation with Clinical and Resection Findings

Debasmita Das[1], Raul Gonzalez[2]
[1]Beth Israel Deaconess Medical Center, Boston, MA, [2]Beth Israel Deaconess Medical Center, Harvard Medical School, Boston, MA

Disclosures: Debasmita Das: None; Raul Gonzalez: None

Background: Pathologists are increasingly asked to evaluate fine-needle biopsy (FNB) specimens, including from pancreas lesions. The challenges of diagnosing pancreatic NET on FNB are not well characterized, nor are the relationships between FNB and clinical or resection findings. We undertook this study to report our experience with a large series of such samples.

Design: We searched our departmental archives for pancreas FNBs diagnosed as NET. Neuroendocrine carcinomas were excluded. For cases with available slides, we recorded specimen cellularity, morphology, and Ki67 immunohistochemical index. We also reviewed pre-biopsy clinical information, and the grade and stage of subsequent resection specimens, when available. FNB and resection findings were compared using the unpaired t-test, with a significance set at $P<0.05$.

Results: We identified 85 pancreatic NET FNB samples from 84 patients (56 men and 28 women with a mean age of 60 years). NET was the leading clinical and imaging diagnosis in only 24 cases (29%). Mean lesion size on imaging was 2.6 cm (range: 0.6-13.4 cm). By histology, 68 cases (80%) were NET not otherwise specified (NOS), while 13 (15%) were sclerosing NETs (Fig 1). Mean specimen cellularity was 20%. NOS cases often yielded bloody specimens, with floating NET cells visible at high power (Fig 2A-B). Lesional cells were often compressed and subtle in sclerosing NETs but became readily visible on neuroendocrine immunohistochemistry (Fig 2C-D). NET subtype did not correlate with imaging size or FNB cellularity. Ki67 stains were available on 73 FNBs (50 grade 1, 21 grade 2, 2 grade 3). Subsequent surgical resection specimens were available for 43 cases (51%). FNB cellularity nearly correlated with resection pT-category stage (mean cellularity 14% for pT1 cases vs. 25% for other cases, $P=0.088$) and pN status (mean cellularity 18% for pNX/pN0 cases vs. 29% for pN1 cases, $P=0.068$). Ki67 stains were available for 38 FNB with matched resections, with 29 (76%) having concordant grades and the other 9 (24%) being upgraded on resection (8 grade 1 to grade 2, 1 grade 2 to grade 3).

Figure 1 - 1118

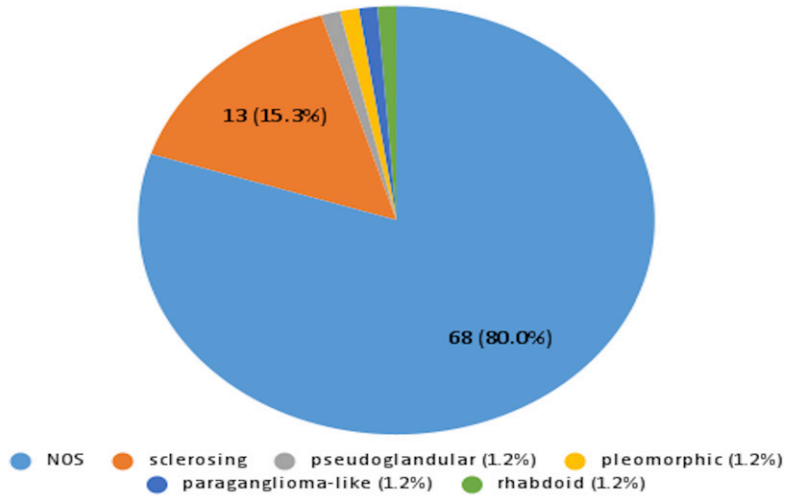

Fig 1: Subtypes of pancreatic NET

Figure 2 - 1118

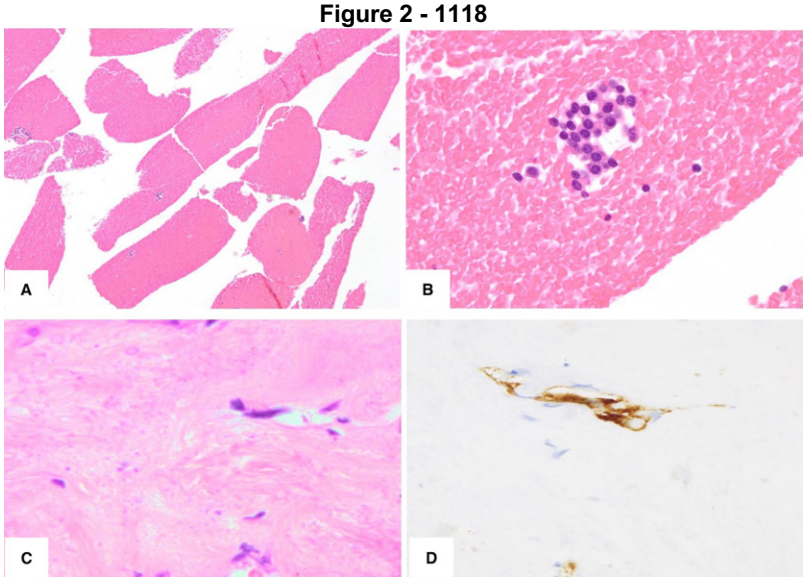

Conclusions: Pancreatic NETs can be encountered on FNB, often appearing bloody/paucicellular or sclerotic. Pathologists should have a high index of suspicion for NET on pancreatic FNB not clearly representing adenocarcinoma, and readily employ neuroendocrine stains to diagnose subtle NETs. Ki67 grading is fairly accurate on FNB and should be performed, though about one-fourth of NETs may be upgraded on resection.

1119 Porcelain Gallbladder May Be in the Spectrum of IgG4 Mediated Diseases: Quantitative Image and Laboratory Data Analysis

Farah El-Sharkawy Navarro[1], Sara Stone[2], Emma Furth[3]
[1]University of Pennsylvania, Philadelphia, PA, [2]Hospital of the University of Pennsylvania, Philadelphia, PA, [3]Perelman School of Medicine, Hospital of the University of Pennsylvania, Philadelphia, PA

Disclosures: Farah El-Sharkawy Navarro: None; Sara Stone: None; Emma Furth: None

Background: Porcelain gallbladder (PGB) is a rare and distinct form of cholecystitis defined by diffuse mural hyalinization and variable calcification whose pathogenesis is unknown. We observed variable plasma cell enrichment in PGB compared to typical chronic cholecystitis, and hypothesized that PGB may be on the spectrum of IgG4-associated diseases.

Design: PGB cases and randomly selected cases of lymphoplasmacytic cholecystitis (LPC) and chronic cholecystitis (CC) were selected from 1992 to 2019. The LPC group was sub-classified into those with autoimmune pancreatitis (AIP) and primary sclerosing cholangitis (PSC). Patients with hepatobiliary and pancreatic malignancy were excluded. Patient demographics, survival, comorbidities, and pre and post cholecystectomy liver function tests (LFTs) were analyzed. H&E slides were scored for calcification and hyalinization (0-3). Slides were stained for CD138 and IgG4, scanned, and the number of CD138+ and IgG4+ cells determined using QuPath image analysis software. The ratio of IgG4/CD138 was calculated for each case and presented as mean ± standard error for each group. Groups were compared using T-test and ANOVA as indicated.

Results: A total of 62 cases were included for analysis: PGB n=35, LPC n=18 (AIP=7 and PSC=11), and CC n=9. The IgG4/CD138 ratio was 0.12 ± 0.02 for PGB, 0.18 ± 0.06 for LPC, and 0.03 ± 0.01 for CC. Within the LPC group, the IgG4/CD138 ratio was 0.38 ± 0.12 for AIP and 0.05 ± 0.02 for PSC. PGB and LPC had a significantly higher IgG4/CD138 ratio than the CC group ($p<0.05$). Significant gallbladder hyalinization and calcification were observed only in the PGB group. Cholelithiasis was present in PGB = 31/35 (89%), LPC = 4/18 (22%), CC = 9/9 (100%). Prior to surgery, LFTs were higher in the PSC subgroup as compared to the other groups and declined significantly post-operatively (Figure 1). There was no correlation of IgG4/CD138 ratio with the degree of hyalinization or calcification in PGB.

Figure 1 - 1119

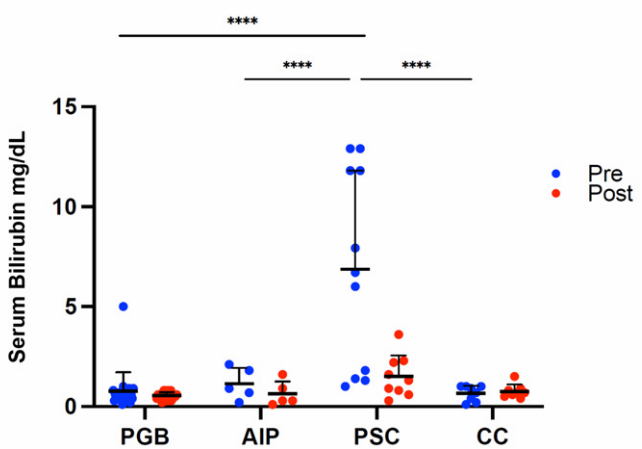

Conclusions: Gallbladder hyalinization, calcification, and high rates of cholelithiasis were seen in PGB as compared to AIP. Increased gallbladder IgG4+ plasma cells and gallbladder wall thickening and fibrosis has been observed in AIP patients, with only rare descriptions of isolated IgG4-related sclerosing cholecystitis. Our finding of increased IgG4/CD138 ratio in PGB suggests that PGB may be a unique manifestation of IgG4 disease in the biliary tree.

1120 Ki67 of >= 10% Identifies an Aggressive Group of PanNETs and Lends Support to Emerging Protocols in Oncology Literature Utilizing This Cut-off for Closer Follow-up and Chemotherapy Candidates

Ozgur Eren, Pelin Bagci, Serdar Balci, Burcu Saka, Cenk Sokmensuer, Can Berk Leblebici, Yue Xue[6], Michelle Reid[7], Orhun Taskin, Yersu Kapran, Claudio Luchini, Aldo Scarpa, Olca Basturk[10], N. Volkan Adsay

[1]Marmara University, Istanbul, Turkey, [2]Independent Consultant, Turkey, [3]Koç University School of Medicine, Istanbul, Turkey, [4]Hacettepe Üniversitesi Tip Fakültesi, Ankara, Turkey, [5]Hacettepe University, Turkey, [6]Northwestern University Feinberg School of Medicine, Chicago, IL, [7]Emory University Hospital, Atlanta, GA, [8]Koç University, Istanbul, Turkey, [9]University of Verona, Verona, Italy, [10]Memorial Sloan Kettering Cancer Center, New York, NY, [11]Koç University Hospital, Istanbul, Turkey

Disclosures: Ozgur Eren: None; Pelin Bagci: None; Serdar Balci: None; Burcu Saka: None; Cenk Sokmensuer: None; Can Berk Leblebici: None; Yue Xue: None; Michelle Reid: None; Orhun Taskin: None; Yersu Kapran: None; Claudio Luchini: None; Aldo Scarpa: None; Olca Basturk: None; N. Volkan Adsay: None

Background: Per guidelines, G1 (Ki67 index, < 3%) and G2 (Ki67 index 3-20%) PanNETs are managed almost identically. However, in the oncology literature, Ki67 index of 10% is increasingly used as the cut-off for selecting patients for chemotherapy and closer follow-up (PMID: 34300189), despite the absence of systematic pathology-based studies supporting this.

Design: Ki67 index was counted in 190 resected PanNETs using the manual count from computer-captured hot spot image (PMID: 25412850), and correlated with clinicopathologic parameters.

Results: Twenty-eight PanNETs (15%) had Ki67 index >= 10%, and 15 of these (overall 7.9% of the cases) were in the G2 category (had index 10-20 %). Signs of aggressiveness (tumor size, perineural/lymphovascular invasion, infiltrative growth pattern) and metastatic (lymph node or liver/distant) behavior were significantly more common in the 10-20% group in comparison to PanNETs with Ki67 3 - <10% (n=70). The former group behaved similarly to PanNETs with Ki67 index > 20% (n=13). See the table for comparative findings. Furthermore, analysis with “maximally selected rank statistics” method revealed the proper Ki67 index cut-off to be 12%.

	Ki-67 (%)				p-value
	G1 < 3 (n = 92)	G2a 3 - < 10 (n = 70)	G2b 10 - 20 (n = 15)	G3 > 20 (n = 13)	
Mean Size in cm (SD)	2.6 (1.9)	4.0 (2.4)	4.3 (2.7)	4.9 (2.6)	0.014
Lymph Node Metastasis	%23.7	%35.5	%73.3	%36.4	0.003
Liver/Distant Metastasis	%7.5	%22.6	%61.5	%45.5	<0.001
Perineural Invasion (PNI)	%16.5	%35.7	%53.3	%46.2	0.002
Lympho-vascular Invasion (LVI)	%23.3	%60.0	%80.0	%92.3	<0.001
Infiltrative pattern score moderate/high	%46.2	%67.3	%84.6	%77.7	<0.001

Conclusions: Among resected PanNETs, those with Ki67% >= 10% (15% of cases) are more aggressive and metastasis-prone. This lends support to evolving management protocols in the oncology literature that regard this group as potential chemotherapy candidates warranting close follow-up (including frequent MRI evaluation of pancreas and liver and NET-specific PET scans). This study highlights the importance of accurate Ki67 index counting and reporting as a numerical unit rather than simple G1/2 which is a heterogenous and broad category. PanNETs with Ki67 indices between 10-20% should be regarded as G2b (aggressive subset of G2), at least conceptually. Additional studies are needed to verify these findings.

1121 The Prognostic Significance of the Station 8a Lymph Regional Node in Resectable Adenocarcinoma of the Pancreatic Head

Daniel Geisler[1], Katelyn Smith[1], Phoenix Bell[1], Patrick Henn[2], Brian Theisen[3], Susan Shyu[1], Aatur Singhi[1]
[1]University of Pittsburgh Medical Center, Pittsburgh, PA, [2]University of Colorado Anschutz Medical Campus, Aurora, CO, [3]Henry Ford Hospital, Detroit, MI

Disclosures: Daniel Geisler: None; Katelyn Smith: None; Phoenix Bell: None; Patrick Henn: None; Brian Theisen: None; Susan Shyu: None; Aatur Singhi: *Consultant*, Foundation Medicine

Background: Regional lymph node status is an important prognostic factor of overall survival (OS) for pancreatic ductal adenocarcinoma (PDAC) patients undergoing pancreaticoduodenectomy (PD) with curative intent. Among regional lymph nodes of the pancreatic head/uncinate, the station 8a lymph node is present along the anteriosuperior aspect of the common hepatic artery and is often harvested during PD. However, the prognostic significance of metastatic spread to the station 8a lymph node is unclear. We, therefore, examined the clinicopathologic features and OS with respect to the status of the station 8a lymph node for PDAC patients.

Design: In total, 595 consecutive PDs with an excised station 8a lymph node were reviewed and assessed for: patient age, gender, neoadjuvant and adjuvant treatment, tumor size, histologic grade, perineural and lymphovascular invasion, T- and N-stage, number of positive lymph nodes, positive lymph node ratio, surgical resection margins, and OS.

Results: Lymph node metastasis was identified for 430 (72%) patients, and 203 (34%) patients had 4 or more positive lymph nodes (pN2). Metastatic disease involving the station 8a lymph node was identified in 82 (14%) cases and, for lymph node-positive patients, station 8a metastasis correlated with larger tumor size, advanced N-stage, greater positive lymph nodes, and a higher positive lymph node ratio ($p<0.02$). In fact, 62 (of 82, 76%) station 8a-positive patients had pN2 disease. The 1- and 3-year OS rates for pN2 patients with and without station 8a lymph node metastasis were 50% and 8%, and 66% and 20%, respectively ($p=0.006$). Based on multivariate analysis, station 8a lymph node metastasis was a negative prognostic factor for OS ($p=0.020$) and was independent of patient age, histologic grade, perineural and lymphovascular invasion, advanced T-stage and N-stage, positive resection margins, and both neoadjuvant and adjuvant therapy. Similarly, among pN2 patients, a positive station 8a lymph node was a negative prognostic factor for OS ($p<0.001$) and was independent of patient age, histologic grade, perineural and lymphovascular invasion, advanced T-stage and N-stage, positive resection margins, and both neoadjuvant and adjuvant therapy.

Conclusions: Station 8a lymph node metastasis for PDAC patients is associated with adverse clinicopathologic features, and an independent predictor of poor patient OS. Thus, a positive station 8a lymph node is prognostically relevant and should be considered when reporting lymph node status.

1122 Inadequacy of Pancreatic Adenocarcinoma Tissue Sampling in the Era of Precision Medicine: A single center experience

Iván González[1], Deanne Yugawa[2], Ankit Chooda[2], James Farrell[2], Gena Foster[2], Nikhil Joshi[2], Nicole Gianino[2], Kurt Schalper[3], Ilke Nalbantoglu[4], Marie Robert[4]
[1]Children's Hospital of Philadelphia, Philadelphia, PA, [2]Yale University School of Medicine, New Haven, CT, [3]Yale University, New Haven, CT, [4]Yale School of Medicine, New Haven, CT

Disclosures: Iván González: None; Deanne Yugawa: None; Ankit Chooda: None; James Farrell: None; Gena Foster: None; Nikhil Joshi: None; Nicole Gianino: None; Kurt Schalper: *Consultant*, Clinica Alemana Santiago, Celgene, Moderna Therapeutics, Shattuck Labs, Pierre-Fabre, AstraZeneca, Dynamo Therapeutics, EMD Serono, Takeda, Torque Therapeutics, Takeda, Agenus and Merck; *Grant or Research Support*, Navigate Biopharma, Tesaro, Moderna Therapeutics, Takeda Pharmaceuticals, Surface Oncology, Pierre-Fabre Research Institute, Merck, Bristol-Myers Squibb, AstraZeneca, Ribon Therapeutics and Eli Lilly; Ilke Nalbantoglu: None; Marie Robert: *Grant or Research Support*, Bristol Myers Squibb; *Consultant*, Takeda, Teva Pharmaceuticals

Background: Diagnostic cancer samples usually consist of small biopsies with priority for the least invasive approach. However, there is a disconnect between diagnostic goals and subsequent expectations for genomic analysis/drug development needs on small samples. This is especially true in pancreas adenocarcinoma (PDAC), where tumor/stroma ratios are low and resection rates are less than 30%, leading to insufficient tissue to support additional tissue inquiries. Definition of sample adequacy for precision medicine are lacking. We evaluated tumor/stroma quantity, and adequacy for subsequent tests in pancreas biopsies over a 30-year period at a single institution.

Design: The Pathology database was searched for initial diagnostic pancreas biopsies from 1990-2020. Following confirmation of PDAC by 3 gastrointestinal pathologists, semi-quantitative assessment of amounts of tumor, stroma, necrosis and benign tissue was performed on each sample at the light microscope. Each element was scored as absent, scant (<33% of tissue area), moderate (33-66%) or abundant (>66%). The number of diagnostic/biomarker immunohistochemical (IHC) stains and tumor genomic profiling (TPL) requests were noted. Institutional review board requirements were fulfilled.

Results: Diagnostic PDAC biopsies from 193 patients were retrieved (see Table 1). In 177(92%) patients, biopsies were obtained via endoscopic ultrasound (EUS) while 16(8%) were CT-guided/surgical. Of EUS biopsies, a 22-gauge needle was employed in 129(74%) patients, a 20-gauge needle in 22(13%) and a range of other needle types in 23(12%). At initial diagnosis, an average of 4(2 – 13) level sections were cut per sample, with diagnostic IHC performed in 49(25%) biopsies. Tumor was scant in 87(45%) and abundant in 49(25%) biopsies, while stroma was scant in 49(25%) and abundant in 71(37%) biopsies. Biomarker/TPL was requested in 45(25%) patients, including MMR(N=31), HER2(N=8), and TPL(N=28). 12/28(43%) TPL tests failed due to inadequate tumor.

Table 1. Patient and biopsy characteristics

	N: 193
Gender, n (%)	
Male	100 (51.8%)
Female	93 (48.2%)
Age, mean (range) (years)	68 (35 – 96)
Tumor location, n (%) (available in 173)	
Uncinate	5 (2.8%)
Head	87 (49.4%)
Neck	10 (5.7%)
Body	39 (22.2%)
Tail	35 (19.9%)
Size, mean (range) (cm) (available in 176)	3.4 (1.2 – 9.8)
Biopsy approach, n (%)	
Endoscopic ultrasound	177 (91.7%)
CT-guided	15 (7.8%)
Open surgery	1 (0.5%)
Type of needle use for endoscopic ultrasound, n (%) (available in 174)	
18-gauge	4 (2.3%)
19-gauge	8 (4.6%)
20-gauge	22 (12.6%)
22-gauge	129 (74.1%)
23-gauge	1 (0.6%)
25-gauge	10 (5.7%)
Number of passes, mean (range)	3.6 (1 – 9)
Concomitant fine-needle aspiration, n (%)	
No	56 (29%)
Yes	137 (71%)
Fine-needle aspiration, n (%)	
Non-diagnostic	1 (0.7%)
Negative for malignancy	2 (1.5%)
Atypical	17 (12.4%)
Suspicious for malignancy	4 (3%)
Positive for malignancy	113 (82.5%)
Number of biopsy levels examined, mean (range)	4 (2 – 13)
Immunohistochemistry performed, n (%)	
No	144 (74.6%)
Yes	49 (25.4%)
Number of IHC performed, mean (range)	3 (1 – 10)
Tumor quantification, n (%)	
Scant	87 (45.1%)
Moderate	57 (29.5%)
Abundant	49 (25.4%)
Desmoplastic stroma quantification, n (%)	
No	2 (1%)
Scant	49 (25.4%)
Moderate	71 (36.8%)
Abundant	71 (36.8%)
Benign pancreatic parenchyma quantification, n (%)	
No	153 (79.3%)
Scant	20 (10.4%)
Moderate	14 (7.3%)
Abundant	6 (3.1%)
Tissue necrosis quantification, n (%)	

No	173 (89.6%)
Scant	9 (4.7%)
Moderate	7 (3.6%)
Abundant	3 (1.6%)
Biomarkers performed, n (%)	
No	148 (75%)
Yes	45 (25%)
MMR proteins adequate for examination, n (%) (n: 31)	
No	1 (3.2%)
Yes	30 (96.8%)
HER2 by IHC adequate for examination, n (%) (n: 8)	
No	1 (2.5%)
Yes	7 (87.5%)
PD-L1 adequate for examination, n (%) (n: 16)	
Yes	15 (93.8%)
No	1 (6.2%)
Tumor profiling testing adequate for examination, n (%) (n: 28)	
No	12 (42.9%)
Yes	16 (57.1%)

Abbreviations: IHC – immunohistochemistry; MMR – mismatch repair; PD-L1 – program death ligand-1.

Conclusions: In a large cohort of PDAC patients, pancreas biopsies, while sufficient for diagnosis, were often inadequate for genomic analysis. Further, there was insufficient tissue to support the development and testing of emerging biomarkers in a tumor urgently in need of effective therapies. As biomarkers and genetic sequencing continue to drive cancer therapy, re-evaluation of current sampling protocols by the interdisciplinary team will be crucial to achieve better survival in the era of personalized medicine.

1123 Genomic Profiling of Pancreatic Ductal Adenocarcinoma, Intrahepatic and Extrahepatic Cholangiocarcinoma

Matthew Gosse[1], Ramakrishna Sompallae[1], Natalya Guseva[2], Anthony Snow[2], Aaron Bossler[2], Deqin Ma[1]
[1]University of Iowa Hospitals & Clinics, Iowa City, IA, [2]University of Iowa, Iowa City, IA

Disclosures: Matthew Gosse: None; Ramakrishna Sompallae: None; Natalya Guseva: None; Anthony Snow: None; Aaron Bossler: None; Deqin Ma: None

Background: In the work up of a carcinoma of unknown primary, the distinction between pancreatic ductal adenocarcinoma (PDC) and cholangiocarcinoma (CCA) is a challenging endeavor due the overlap in morphology and lack of immunohistochemistry (IHC) markers. The distinction has important ramifications for treatment and prognosis. Genomic analyses of these tumor types have been described. Intra- and extra-hepatic cholangiocarcinoma (iCCA and eCCA) had distinct molecular profiles. iCCA are enriched in *IDH1/2* and *BAP1* mutations and *FGFR2* fusions whereas eCCA and PDC had a higher rate of *TP53* and *KRAS* mutations. In this study, we directly compared molecular profiles of our institutional cohort of iCCA, eCCA, and PDC to aid in the distinction of the diagnosis of these neoplasms.

Design: Sixty-one cases (39 PDC, 12 iCCA, and 10 eCCA) were tested using a custom-designed 213-gene next generation sequencing panel. For detection of gene fusions, the commercially available FusionPlex CTL panel (ArcherDx) was used. Total nucleic acid extracted from microdissected, formalin-fixed, paraffin-embedded tissue was used to generate NGS libraries and sequencing was performed on Illumina NextSeq. Data were analyzed using the BWA and Pisces v2 (Illumina) for variant calling, ArcherDx software for fusion, and an in-house built custom pipeline for copy number variation (CNV).

Results: The demographics of the cohort are shown in Table 1. Somatic mutations detected in all tumors are summarized in Fig. 1. Mutations in *IDH1* and *BAP1*, and *FGFR2* fusions were most commonly detected in iCCA; eCCA and PDC shared a similar mutation profile of *TP53* and *KRAS* variants present in 70-80% of cases. *KRAS* G12R (9) and Q61H (3) were only detected in PDC; G12C in 2 eCCA, and G13D in 1 iCCA (Fig. 2). Gene rearrangements were detected in 4/11 iCCAs (3 with *FGFR/BICC1* and 1 with *FGFR/ SORBS1*). No fusions were detected in eCCA (10) or PDC (32). CNV analysis showed *CDKN2A/B* loss in 18% PDC (n=39), 1 eCCA (n=12) and none in iCCA (n=10). All 4 iCCAs with *BAP1* mutations showed BAP1 lost by IHC and all 4 cases of intact BAP1 expression by IHC showed no *BAP1* mutation.

Table 1. Demographics of cases tested

	iCCA	eCCA	PDC
Number of cases	12	10	39
Age	64.5	73	71
Gender			
Female	6	5	19
Male	6	5	20
Stage			
1	2	1	5
2	2	5	11
3	5	2	8
4	3	2	15

iCCA, Intrahepatic cholangiocarcinoma; eCCA, extrahepatic cholangiocarcinoma; PDC, pancreatic duct adenocarcinoma.

Figure 1 - 1123

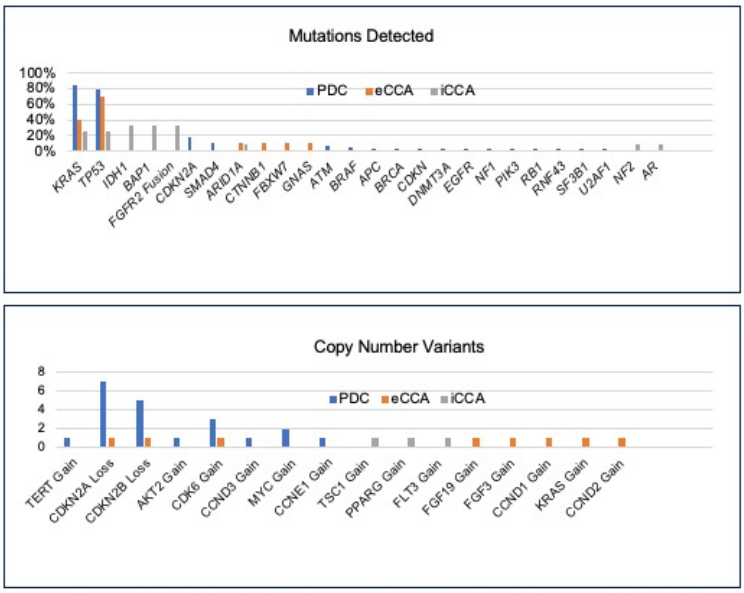

Figure 1. Mutation and copy number variants detected by next generation sequencing assay. Top: Mutations detected; Bottom: Copy number variants identified.

Figure 2 - 1123

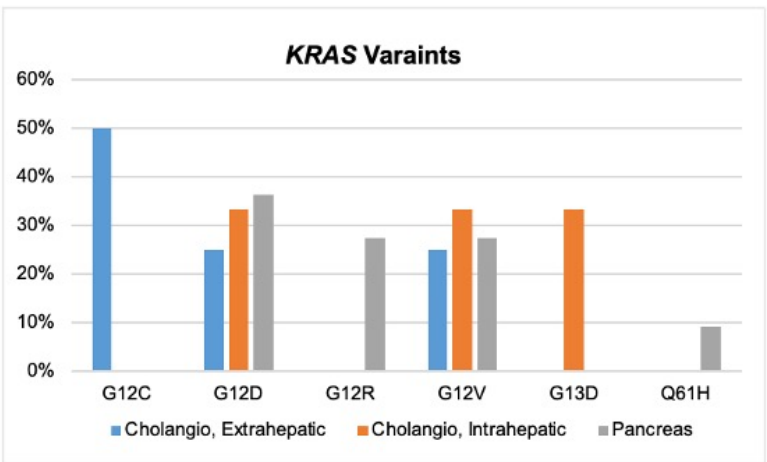

Figure 2. *KRAS* variants detected by NGS.

Conclusions: Our data show that the presence of *IDH1*, *BAP1* mutation and *FGFR2* fusion supports the diagnosis of iCCA. Tumors with loss of *CDKN2A/B* and/or *SMAD4* and *ATM* mutations were most likely PDC. Our results support the previous molecular findings in CCA and PDC. The difference in *KRAS* variants in these two tumor types observed in this small cohort also warrants further investigation.

1124 Clinicopathologic Spectrum of Pancreaticobiliary Neoplasms in Patients with Germline BRCA1/2 Mutations

Christian Hirt[1], Andy Silva-Santisteban Merino[1], Mandeep Sawhney[1], Monika Vyas[1]
[1]Beth Israel Deaconess Medical Center, Harvard Medical School, Boston, MA

Disclosures: Christian Hirt: None; Andy Silva-Santisteban Merino: None; Mandeep Sawhney: None; Monika Vyas: None

Background: Patients with germline mutations in BRCA1/2 genes are known to have an increased risk of pancreatic and biliary tract cancer. Sampling of small pancreaticobiliary masses during surveillance often yields very limited material which is often difficult to classify. The aim of this study was to characterize the clinicopathologic spectrum of BRCA1/2 associated neoplasms which would direct pathologists in identifying these neoplasms and streamlining their work up.

Design: The pathology and surveillance database were reviewed for pancreaticobiliary pathology samples from patients with germline BRCA1/2 mutations. The demographic information (age, sex), history of malignancy, radiologic features, genetic testing results and patient follow up were recorded. The H&E and any immunohistochemical stained slides were reviewed and final diagnosis was recorded.

Results: 16 patients (13 BRCA2 (81.3%), 3 BRCA 1 (18.7%)) were identified among 502 patients (3.1%), including 11 females and 5 males (average age 64.9, range: 38-78 years). The primary sites included; pancreas (13, 81.25%), ampulla (2, 12.5%) and common bile duct (n=1, 6.2%). 7 patients had prior history of one or more malignancy (6 breast, 1 each of adnexal, stomach, skin, and lung). On imaging (n=15), the lesions appeared solid, hypoattenuating (12, 80%), cystic (2, 13.3%) and duct narrowing (1, 6.6%). The pancreatic primary neoplasms included ductal adenocarcinoma (PDAC) (5, 31%), acinar cell carcinomas (n=2, 12.5%), poorly differentiated carcinoma (n=2, 12.5%), well differentiated neuroendocrine tumors (NET) (n=2, 12.5%), intraductal papillary mucinous neoplasms (n=1, 8.3%) and benign cyst (n=1, 8.3%). The poorly differentiated carcinoma also showed a SMARCB1 mutation on tumor profiling. 4 (25%) patients had nodal metastases and 3 (18.7%) patients had liver metastases. Average follow up period was 30.4 months. 6 patients (3 PDAC, 1 IPMN, 1 NET, 1 benign cyst) had no evidence of disease while 8 patients were either died or were alive with disease and 2 lost in follow up.

Figure 1 - 1124

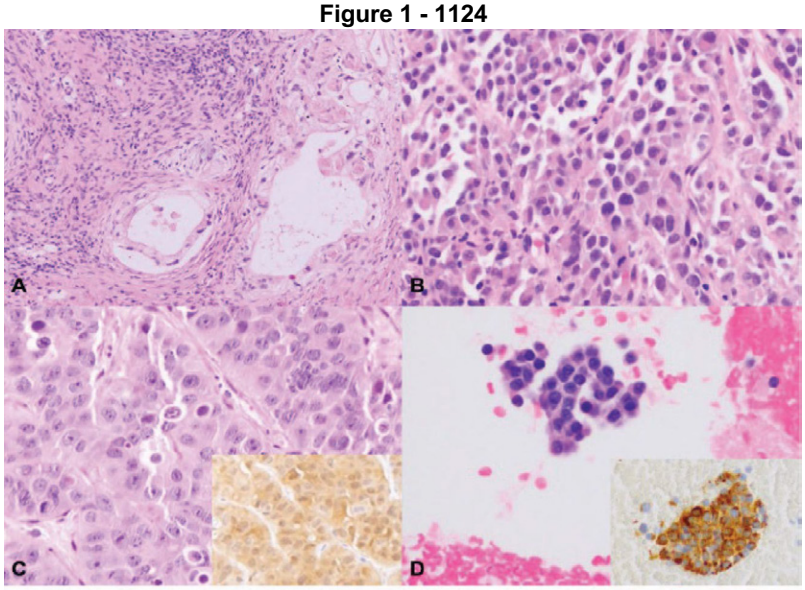

Examples of pancreatic neoplasms in patients with a germline BRCA1/2 mutation.
A: Pancreatic ductal adenocarcinoma.
B: Poorly differentiated carcinoma.
C: Acinar cell carcinoma (inset - BCL10 immunohistochemistry).
D: Well-differentiated neuroendocrine tumor (inset - chromogranin immunohistochemistry).

Conclusions: We describe the clinicopathologic spectrum of pancreaticobiliary neoplasms in a cohort of 16 patients with germline BRCA1/2 mutations. The primary site in these patients is not limited to pancreas and includes the ampulla and biliary tract. While most the common histologic subtype is PDAC, acinar cell carcinoma and neuroendocrine neoplasms must be considered in the differential diagnoses.

1125 Targeted Genomic Profiling of Gallbladder Carcinoma

Nuzhat Husain[1], Sridhar Mishra[1], Swati Kumari[1], Pallavi Srivastava[1], Anshuman Pandey[1], Saumya Shukla[1]
[1]Dr Ram Manohar Lohia Institute of Medical Sciences, Lucknow, India

Disclosures: Nuzhat Husain: None; Sridhar Mishra: None; Swati Kumari: None; Pallavi Srivastava: None; Anshuman Pandey: None; Saumya Shukla: None

Background: Gallbladder cancer (GBC) often presents in late stage of disease with poor prognosis. Mutations for selection of targeted therapies are limited. Next-generation sequencing (NGS) using frequently mutated genes for GBC may provide a reference for clinical management. The current study identifies cancer-related genetic alterations by NGS in cases of GBC and their association with clinicopathological features.

Design: DNA from FFPE tissue of 37 cases of GBC was sequenced to high depth, uniform coverage (ION, Personal Genome Machine) and analysed for genomic alterations using a 22 gene panel related to colorectal cancer. The germline variants were filtered using variant calls from blood and non-tumor control samples.

Results: A total of 178 alterations were identified for an average of 4.8 alterations per tumor (range 1–15). A total of 38 different genomic alterations with the potential to personalize therapy in SMAD4 (60.60%), NOTCH1 (45.45%), ERBB2 (45.45%), PIK3CA (33.33%) and MET (30.30%), PTEN (30.30%), EGFR (24.24%), KRAS (21.21%), BRAF (9.09%) and NRAS (6.06%) gene. In 66.67% (2/3) co-mutated cases lymph node metastasis was not evident. BRAF gene mutation was mutually exclusive with PIK3CA, TP53 (n=3/3) and EGFR in 2/3 patients. Hot spot mutations of EGFR, KRAS and NRAS as seen in colorectal cancers were also observed in GBC (Table 1).Table 1 further details coexisting mutations. KRAS mutation was observed in 3/8 in EGFR positive cases. TP53 mutation was associated with histopathological differentiation (p=0.0001), ERBB4 & ALK mutation was associated with necrosis (p=0.012, 0.027), EGFR mutation was associated with mucinous tumors (p=0.023) and ERBB2 gene mutation was associated with T stage (p=0.036). No significant correlation of genetic profile with lympho-vascular invasion, perineural invasion, lymph-node metastasis was observed.

Table 1: Hot spot gene mutation of EGFR, KRAS and NRAS

Exon	Genotype	AA change	Other associated pathogenic mutations
EGFR			
19	c.2236G>A	p.Glu746Lys	ERBB4, SMAD4, TP53, FBXW7
19	c.2227G>A	p.Ala743Thr	PTEN, NOTCH1, TP53
18	c.2092G>A	p.Ala698thr	ERBB2, NOTCH1, TP53, SMAD4, MET, PTEN, PIK3CA, FGFR1, KRAS, ALK
19	C.2252C>T	p.Thr751Ile	ERBB2, NOTCH1, SMAD4, TP53, MET
18	c.2156G>A	p.Gly719Asp	ERBB4, ERBB2, TP53, PIK3CA, STK11, FBXW7, CTNNB1, FGFR3, KRAS, NRAS, ERBB2
20	c.2369C>T	p.Thr790Met	ERBB4, ERBB2, TP53, PIK3CA, STK11, DDR2, CTNNB1, FGFR3, BRAF
18	c.2092G>A	p.Ala698Thr	SMAD4, PTEN, TP53, PIK3CA, AKT11, DDR2, FGFR3, ALK
19	c.2193G>A	p.Trp731Ter	PTEN, TP53, PIK3CA, STK11, CTNNB1, KRAS, NRAS
KRAS mutation			
2	c.40G>A	p.Val14Ile	TP53, ERBB4, CTNNB1
2	c.40G>A	p.Val14Ile	TP53, SMAD4, ERBB2, NOTCH1, EGFR, MET, PTEN
2	c.35G>A	p.Gly12Asp	TP53, ERBB2, NOTCH1, SMAD4, MET, DDR2
2	c.35G>A	p.Gly12Asp	TP53, PIK3CA, MET, DDR2, ALK
2	c.32C>T	p.Ala11Val	TP53, SMAD4
4	c.413G>A	p.Gly138Glu	TP53, ERBB2, ERBB4, NOTCH1, SMAD4, , PIK3CA, STK11, FBXW7, CTNNB1, FGFR3, EGFR, NRAS
2	c.38G>A	p.Gly13Asp	TP53, PTEN, PIK3CA, STK11, CTNNB1, EGFR, NRAS
NRAS mutation			
3	c.181C>A	p.Gln61Lys	PTEN, STK11, CTNNB1, EGFR, KRAS, PIK3CA
11	c.1397G>A	p.Gly466Glu	TP53, FGFR3, STK11, DDR2, AKT1, PIK3CA, ERBB2, CTNNB1, EGFR

Figure 1 - 1125

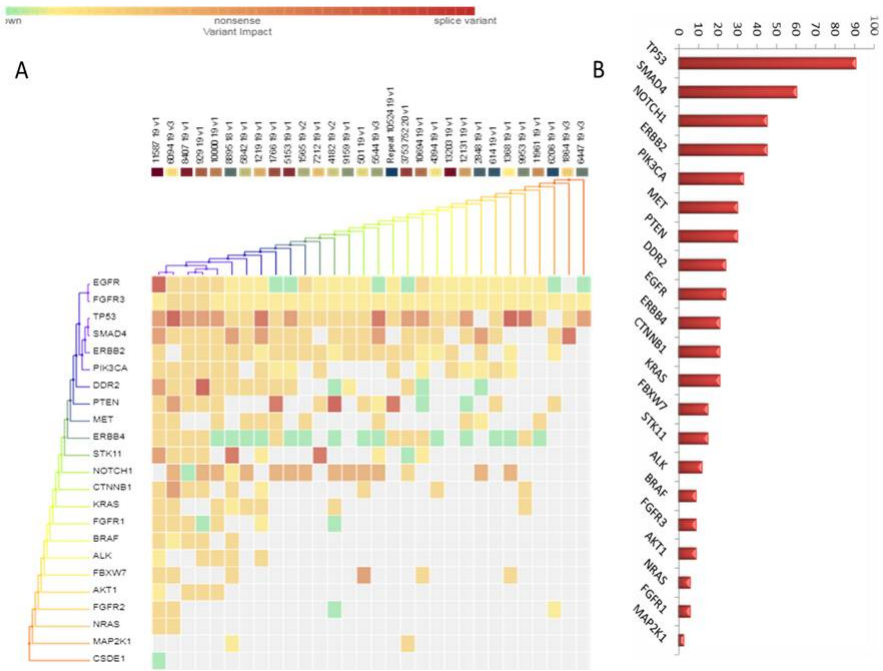

Conclusions: The current study provides an overview of genetic alterations and pathways involved in gallbladder tumorigenesis. Targetable mutations were identified in 89.91% cases and included SMAD4, NOTCH1, ERBB2&4, PIK3CA, MET, PTEN, EGFR, KRAS, BRAF and NRAS and were overlapping those of colorectal carcinoma. The study supports the possible use of genetic profiling and targeted therapy along lines of colorectal cancer.

1126 High Tumor Mutational Burden Identifies Specific Subsets of Pancreatic Cancer Patients with Prolonged Survival and Improved Anti-tumor Immunity

Eva Karamitopoulou-Diamantis[1], Andreas Andreou[2], Anna-Silvia Wenning[3], Beat Gloor[2], Aurel Perren[4]
[1]Institute of Pathology, University of Bern, Bern, Switzerland, [2]Insel University Hospital, University of Bern, Bern, Switzerland, [3]Inselspital University Hospital Bern, Bern, Switzerland, [4]University of Bern, Bern, Switzerland

Disclosures: Eva Karamitopoulou-Diamantis: None; Andreas Andreou: None; Anna-Silvia Wenning: None; Beat Gloor: None; Aurel Perren: None

Background: Tumor Mutational Burden (TMB), defined as the number of somatic mutations per megabase (mut/Mb), can predict the efficacy of immunotherapy, which led to FDA approval of pembrolizumab for TMB-high (≥10 mut/Mb) tumors. Immunotherapy in pancreatic ductal adenocarcinoma (PDAC) has largely focused on patients with microsatellite instable (MSI-high) tumors. Identifying microsatellite stable (MSS) PDACs with high TMB might expand the number of patients that could benefit from immunotherapy.

Design: We assessed TMB in 120 conventional, MSS PDACs by using the Oncomine Tumor Mutation Load Assay (ThermoFisher) and the Comprehensive Cancer Panel. 25 (MSS) long-term survivors (LTS, overall survival (OS)>60 months) and five MSI-high cases were assessed in parallel. Cases were divided in TMB-high and TMB-low categories by using a cutoff of 10mut/Mb. Additionally, 12 TMB-high and 15 TMB-low cases were immunoprofiled by multiplex immunofluorescence (CD3, CD4, CD8, FOXP3, CD20, CD68, PD-1, PD-L1, DC-LAMP) followed by automated image analysis.

Results: Median and mean TMB values were 3.36 and 5.64 respectively. Overall, 12 TMB-high cases (median:14.025, range:10.21-129) were detected. They comprised all five MSI-high cases (100%), five LTSs (20%) and two conventional MSS PDACs (1.66%). TMB-high PDACs exhibited high T cell density and significantly increased $CD3^+CD4^+FOXP3^-$T cells (P=0.0398) and DC-$LAMP^+$dendritic cells (DC; P=0.0093), compared with TMB-low cases. Five TMB-high cases (41.66%) were also PD-

L1$^+$ exhibiting various PD1/PD-L1 staining patterns. *ARID1A*- and *ERBB3*-alterations were more frequent in TMB-high tumors. The OS of TMB-high cases ranged between 5-71 months (median:27), whereas that of the TMB-low cases between 3-161 months (median:13), P<0.001.

Figure 1 - 1126

Stromal Immune Cell Types

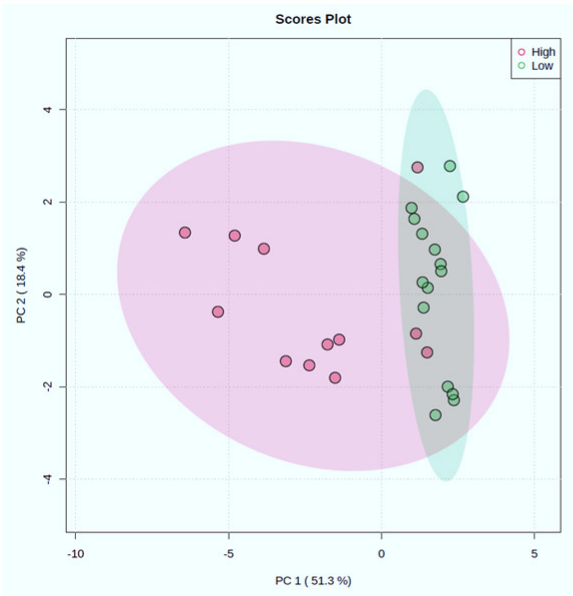

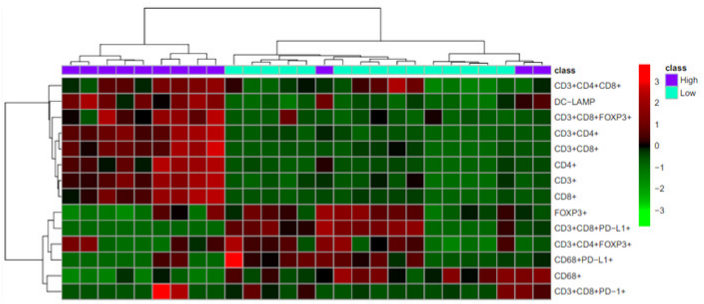

Markers	P Values
DC-LAMP+	1.61E-06
CD4+	2.42E-05
CD3+CD4+	0.00036348
CD3+CD8+	0.0047636
CD8+	0.00071066
CD3+	0.00071066
CD3+CD8+FOXP3+	0.0073537
CD68+	0.027454
CD68+CD206+	0.034391

Conclusions: High TMB mostly identifies patients from specific PDAC-subsets such as LTS (MSS) and MSI-high cases. Their microenvironment displays strong anti-tumor immune response, mediated by increased DC counts, which have the capacity to initiate and regulate T cell responses, as well as CD3$^+$CD4$^+$FOXP3$^-$T cells, known to exhibit direct cytotoxicity against tumor cells as well as potentiate the DCs. TMB-high PDACs frequently harbor other actionable alterations, such as defective mismatch repair (MSI) and DNA Damage Response and Repair (*ARID1A*), as well as *ERBB3*-alterations. These results suggest that PDAC-patients with TMB-high tumors might be good candidates for combinatorial treatments including immunotherapy.

1127 Neoadjuvant Chemotherapy Significantly Alters the Tumor Immune Microenvironment and Stroma Composition in Pancreatic Ductal Adenocarcinoma

Ning Li[1], Qiqi Yu[2], Yongjun Liu[3], Xiaofei Zhang[4]
[1]University of Wisconsin Hospital and Clinics, Madison, WI, [2]Johns Hopkins University School of Medicine, Baltimore, MD, [3]University of Wisconsin School of Medicine and Public Health, Madison, WI, [4]University of Wisconsin, Madison, WI

Disclosures: Ning Li: None; Qiqi Yu: None; Yongjun Liu: None; Xiaofei Zhang: None

Background: Pancreatic ductal adenocarcinomas (PDAC) is generally refractory to immunotherapy due to its immunosuppressive tumor microenvironment (TME). Recently, neoadjuvant chemotherapy (NACT) is increasingly used to improve the resectability and survival of PDAC. In this study, we aim to histologically characterize the effect of NACT on the tumor immune microenvironment (TIME) and stroma composition of PDAC which may alter the antitumor immunity.

Design: Thirty-four PDAC cases which received NACT before surgery (16M/18F, 68.3±2.1 yo) and 26 stage-matched PDAC cases which had upfront surgery without NACT (19M/7F, p=0.1; 66.1±1.4 yo, p=0.4) were retrospectively analyzed. Early and mature tertiary lymphoid structures (eTLS and mTLS) are counted at both the center and the periphery of tumors. Tumor associated neutrophils (TANs) are semi-quantitatively scored on the scale of 0-3 (0, no TANs; 1, rare TANs; 2, apparent TANs; and 3, marked TANs with neutrophilic aggregates). The percentages of collagen rich stroma vs fibroinflammatory stroma are estimated from the most representative tumor areas. Statistical analysis was performed using two-tailed Fisher exact test or student *t* test.

Results: In NACT group, the CA19-9 level is decreased (1360±273 to 116±49 U/mL, p<0.0001) and the Neutrophil-to-Lymphocyte ratio (3.7±0.6 to 7.0±1.8, p=0.06) is increased right after NACT. There is no significant change of the systemic Immune-Inflammation Index (SII). Compared with non-NACT group, the NACT group has significantly lower tumor-to-stromal ratio (36.5±1.7% vs 52.0±2.4%, p<0.001). While the TLS at the periphery of the tumor is significantly decreased (4.5±0.9 vs 9.7±1.1, p<0.001) in NACT group, the intra-tumoral TLS is comparable between two groups (1.3±0.5 vs 0.9±0.4, p=0.54). The number of cases with apparent and marked TANs (score 2 or 3) in NACT group is significantly fewer than non-NACT group (11/34 vs 19/26, p<0.01). Compared to non-NACT group, collagen rich stroma is more common in NACT group (16/34 vs 4/26, p<0.05), while vascular and/or nerve hypertrophy is less common (6/34 vs 15/26, p<0.01).

Conclusions: Our results demonstrated that NACT can significantly alter the TIME by decreasing peritumoral TLS and TAN. It can also alter the stroma topography of PDAC. Multiplexed morphometry quantification is ongoing for a comprehensive immune profiling. Clinical studies are warranted to investigate the impact of these alterations on prognosis. New therapies targeting the altered TME/TIME may offer more promising therapeutic avenues when combined with NACT and surgery.

1128 Loss of PTEN and Expression of GLUT1 Predict the Metastatic Progression of Pancreatic Neuroendocrine Tumors

Azfar Neyaz[1], Jasmijn Westendorp, Abigail Wald[1], Marina Nikiforova[1], Seung-Mo Hong, Christopher Heaphy[4], Lodewijk Brosens[5], Aatur Singhi[1]

[1]University of Pittsburgh Medical Center, Pittsburgh, PA, [2]University Medical Center Utrecht/Amsterdam University Medical Center, Heidelberglaan, Netherlands, [3]Asan Medical Center, Songpa-gu, South Korea, [4]Boston University School of Medicine, Boston, MA, [5]University Medical Center Utrecht, Utrecht, Netherlands

Disclosures: Azfar Neyaz: None; Jasmijn Westendorp: None; Abigail Wald: None; Marina Nikiforova: None; Seung-Mo Hong: None; Christopher Heaphy: None; Lodewijk Brosens: None; Aatur Singhi: None

Background: Pancreatic neuroendocrine tumors (PanNETs) are a heterogeneous group of neoplasms with increasing incidence and unpredictable clinical behavior. Immunohistochemical studies have found loss of expression for ATRX/DAXX to be associated with several adverse prognostic features including early relapse-free survival (RFS). Genomic alterations in *PTEN* and *VHL* have also been implicated in the prognosis of PanNETs, but have not been comprehensively evaluated. We, therefore, analyzed the status of *PTEN* and *VHL* using a large cohort of primary PanNETs and correlated with several prognostic features and RFS.

Design: To assess for *PTEN* and *VHL* genomic alterations, loss of PTEN protein expression and protein expression of GLUT1, respectively, were used as surrogate biomarkers. Immunohistochemical stains for PTEN and GLUT1 were validated using 10 PTEN-mutant and 10 VHL-mutant PanNETs that were genetically confirmed using a targeted next-generation sequencing panel (PancreaSeq). In total, 360 sporadic, primary PanNETs were evaluated for PTEN and GLUT1, and correlated with patient age, gender, tumor size, WHO grade, lymphovascular and perineural invasion, T- and N-stage, status of ATRX/DAXX, synchronous and metachronous distant metastases, and RFS.

Results: Aberrant expression of PTEN, GLUT1, or both proteins were seen in 46 (13%), 43 (12%), and 17 (5%) PanNETs. Both loss of PTEN and overexpression of GLUT1 correlated with large tumor size, high WHO grade, advanced T-stage, loss of ATRX/DAXX, and presence of synchronous and metachronous metastases (p<0.02). Among 271 patients without synchronous metastasis, the 5-year RFS rate for PTEN-negative and/or GLUT1-positive patients was 40% as compared to 89% for PTEN-positive/GLUT1-negative patients (p<0.01). By multivariate analysis, aberrant expression for PTEN and/or GLUT1 was a negative prognostic factor for RFS, and independent of tumor size, WHO grade, lymphovascular and perineural invasion, N-stage, and ATRX/DAXX loss (p<0.01). Moreover, aberrant expression of PTEN, GLUT1, and/or ATRX/DAXX was associated with 5-year RFS rate of 47% as compared to 94% for patients without aberrant expression for these proteins (p<0.01), and remained an independent, negative prognostic factor for RFS (p<0.01).

Conclusions: Loss of PTEN and expression of GLUT1 in PanNETs represent prognostic biomarkers of poor patient outcome; thus, genomic alterations in *PTEN* and *VHL* may play a significant role in PanNET pathogenesis.

1129 TPPP-BRD9 Fusion-Related Gallbladder Carcinomas are Associated with Intracholecystic Neoplasia, Neuroendocrine Carcinoma and a Distinctive Small Tubular-Type Adenocarcinoma Commonly Accompanied with Syringomatous Pattern

Burcin Pehlivanoglu[1], Jill Koshiol[2], Scott Lawrence[3], Juan Araya[4], Serdar Balci[5], Jesper Andersen[6], Catterina Ferreccio[7], N. Volkan Adsay[8]

[1]Dokuz Eylul University, Izmir, Turkey, [2]National Cancer Institute, Rockville, MD, [3]Division of Cancer Epidemiology and Genetics, National Cancer Institute, Bethesda, MD, [4]Universidad de La Frontera, Temuco, Chile, [5]Independent Consultant, Turkey, [6]University of Copenhagen, Copenhagen, Denmark, [7]Pontifica Universidad Católica de Chile, Santiago, Chile, [8]Koç University Hospital, Istanbul, Turkey

Disclosures: Burcin Pehlivanoglu: None; Jill Koshiol: None; Scott Lawrence: None; Juan Araya: None; Serdar Balci: None; Jesper Andersen: None; Catterina Ferreccio: None; N. Volkan Adsay: None

Background: Histopathology can provide important insights as the molecular basis of gallbladder cancer (GBC) is beginning to be unraveled.

Design: In RNAseq analysis, we identified 16 GBCs that harbored a fusion between tubulin polymerization-promoting protein (*TPPP*), a regulatory cytoskeletal gene, and the chromatin remodeler, bromodomain-containing protein 9 (*BRD9*). This fusion, previously noted in <5% of non-small cell lung carcinomas (PMID: 27066085), was called by ≥2 algorithms in 7 patients and verified by Sanger sequencing in 1 (PMID: 33276026).

Results: Most were females (F:M=7:1). 12 were Chinese and 4 were from Chile. Carcinoma identified in the slides corresponding to the molecularly analyzed tissue was in-situ in 2 and invasive in 11/16, and showed the following findings: 1) Intracholecystic neoplasm (ICN): 7/15, (47% vs. 7% in our GBC database, p<0.001), all with gastro-pancreatobiliary phenotype (Fig.1A), often with clear cell change (Fig.1B), and extensive HGD, except 2. 2) Neuroendocrine Carcinoma (NEC): 3 cases (27% vs. 4.6% in our GBC database, p=0.001) showed sheet-like and nested/trabecular growth of monotonous cells with salt-and-pepper chromatin characteristic of NECs. Two were large cell type with prominent clear cell features (Fig.1C), a rare finding in GBNECs; one had relatively bland well-differentiated morphology (Fig.1D), and one had small-cell-like features. 3) A distinctive type of adenocarcinoma: 8 cases revealed a distinctive type of adenocarcinoma composed of widely separated small, round tubular units with relatively uniform nuclei and single prominent nucleoli (Fig.2A). In foci where the glands formed luminal structures, they often exhibited hobnail-like arrangement and apical snouts, reminiscent of tubular carcinomas of the breast (Fig.2B-C). Slightly larger tubules typically had necrotic debris in their lumen, which, combined with the attenuation of the cells and the formation of comma or elongated shapes of the glands with irregular contours created a peculiar syringomatous appearance (Fig.2D). In addition to this pattern, 1 had focal glomeruloid pattern, 1 cribriform arrangement, and 1 kaposiform sarcomatoid component.

Figure 1 - 1129

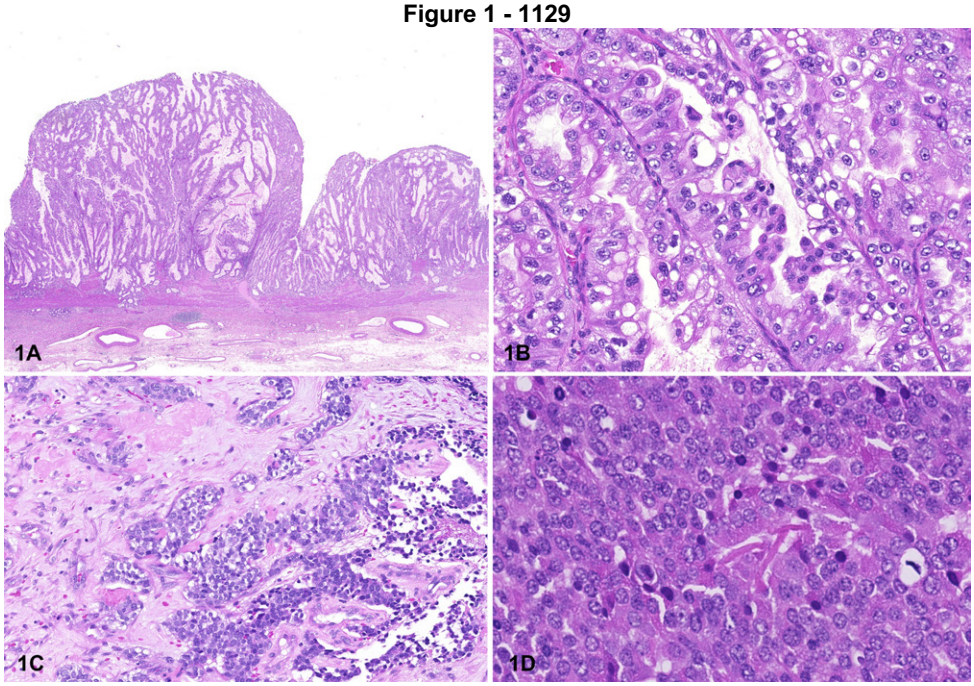

Figure 2 - 1129

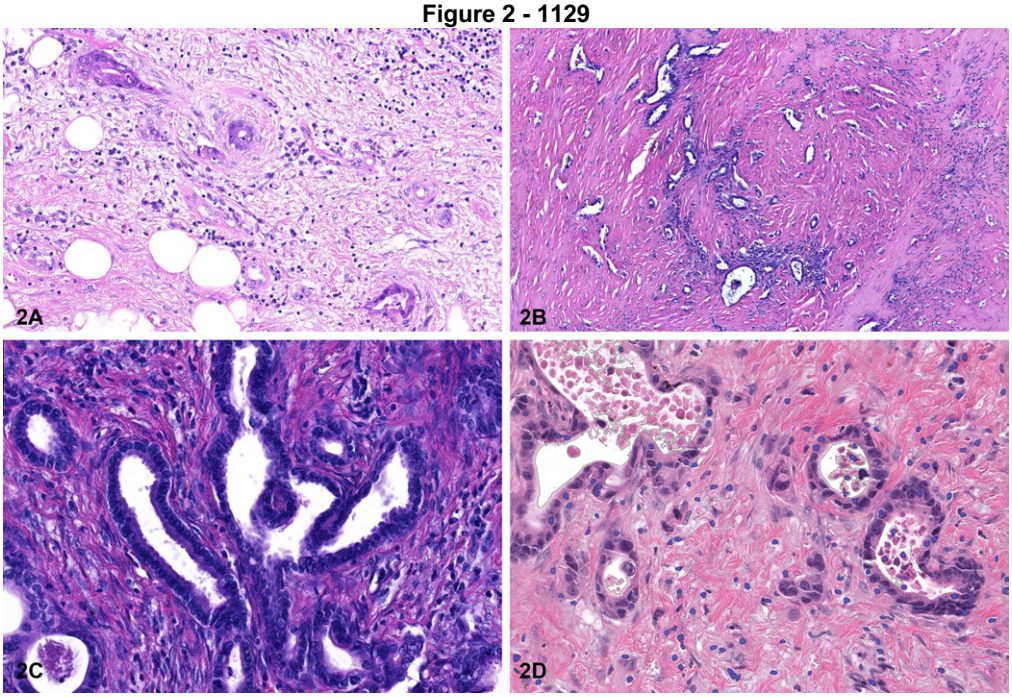

Conclusions: *TPPP-BRD9* fusion-related GBCs often develop through ICNs (adenoma-carcinoma sequence), and appear to be more prone to form neuroendocrine carcinoma. Invasive adenocarcinomas that arise in this setting display a distinctive appearance that we provisionally propose to refer as *TPPP-BRD9* fusion-pattern of GBC until its nature and associations are better clarified.

1130 ERO1L Expression as a Novel Predictor of Poor Prognosis in Resected Pancreatic Ductal Adenocarcinomas

Christine Pesoli[1], Chirag Patel[1], Sameer Al Diffalha[1], Deepti Dhall[1], Sooryanarayana Varambally[1], Upender Manne[1], J. Bart Rose[1], Goo Lee[1]
[1]*The University of Alabama at Birmingham, Birmingham, AL*

Disclosures: Christine Pesoli: None; Chirag Patel: None; Sameer Al Diffalha: None; Deepti Dhall: None; Sooryanarayana Varambally: None; Upender Manne: None; J. Bart Rose: None; Goo Lee: None

Background: Endoplasmic reticulum oxidoreductase 1-alpha (ERO1L) is involved in protective mechanism against endoplatmic reticulum stress. Increased expression have been reported in a variety of human carcinomas and known to be associated with decreased survival in pancreatic ductal adenocarcinomas (PDACs) by TCGA data. We evaluated ERO1L expression in PDACs by immunohistochemistry (IHC) and studied its association with clinico-pathologic features and survival.

Design: ERO1L IHC was evaluated on tissue microarray constructed for 189 resected PDACs. Cytoplasmic and perinuclear staining was considered positive. ERO1L was semi-quantitatively graded using an H-score: the percentage of positive tumor cells (0 to 100%) at each staining intensity (see formula below) were determined and H-score was calculated using the following formula: [no expression(0)x % cells+ weak(1)x % cells+ moderate(2)x % cells+ strong(3)x % cells (final score:0-300)]. H-score 0-100 was considered grade 1 (G1), 101-200 grade 2 (G2), and 201-300 grade 3 (G3). G3 was considered high expression (HE). Strong perinuclear staining >10% of tumor cells (PN>10) was investigated for a simplified assessment. Univariate Kaplan-Meier with log-rank test and multivariate Cox proportional-hazard regression model were performed to estimate overall survival (OS).

Results: The distribution of H-score for the carcinomatous epithelium was as follows: G1: 19%, G2: 49%, G3 (HE): 32%. PN>10 was seen in 58% of all PDACs, 11% in G1, 42% in G2, and 99% in G3. ERO1L is not expressed in normal ductal epithelium and low grade PAN-IN. In univariate analysis, HE [HR: 2.6, 95% CI: 1.8-3.7, p<0.001], PN>10 [HR: 3.9, 95% CI: 2.6-5.8, p<0.001], positive lymph node (LN+) [HR: 2, 95% CI: 2.6-5.8, p<0.001], poorly differentiated carcinoma [HR: 2.9, 95% CI: 1.4-5.7, p=0.003], and perineural invasion (PNI) [HR: 2.14, 95% CI: 1.3-3.5, p=0.002] are associated with decreased OS. Multivariate analysis showed that PN>10, LN+, and PNI were statistically significant risk factors for OS [PN>10: HR: 3.2, 95% CI: 2.0-5.2, p<0.001; LN+:

HR: 2, 95% CI: 1.3-2.9, p<0.001; PNI: HR: 1.7, 95% CI: 1-2.9, p=0.0046]. Median OS for all patients was 25 months (m) with a median of 20m follow-up. Median OS for PN>10 vs PN<10 was 17m and 47m (p<0.001), for HE vs G1+G2 was 16m and 31m (p<0.001), and LN+ vs LN- was 22m and 36m (p<0.001).

Figure 1. ERO1L immunohistochemistry on pancreatic ductal adenocarcinoma tissue microarray. A: Grade1; H score= (0x10%) + (1x90%) + (2x0%) + (3x0%)=90. B: Grade 2; H score= (0x0%) + (1x30%) + (2x60%) + (3X10%)=180. C: Grade 3; H score= (0x0%) + (1X0%) + (2x10%) + (3x90%)=290.

Figure 1 - 1130

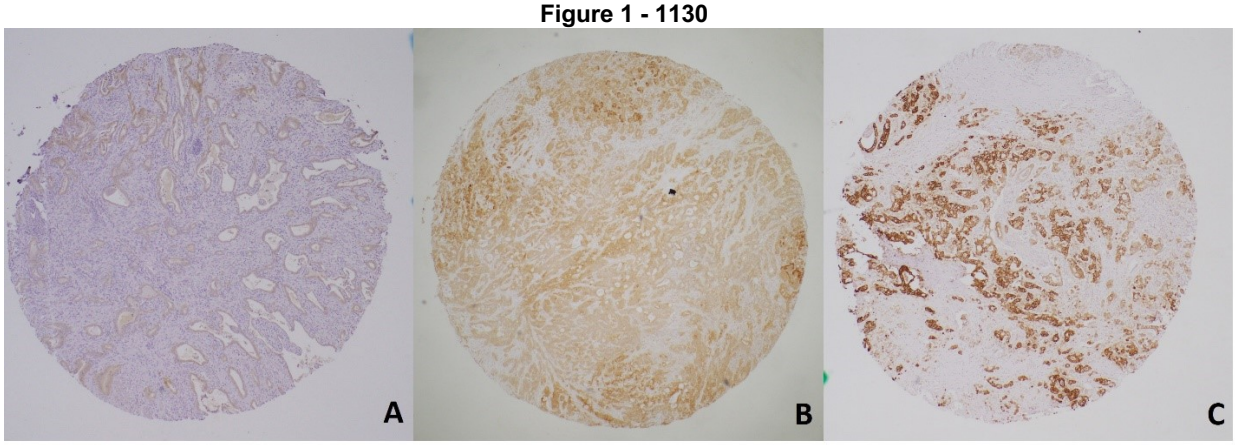

Conclusions: ERO1L overexpression with high H-score and strong perinuclear expression in resected PDACs may serve as an independent prognostic biomarker.

1131 Patterns of Intraparenchymal Spread of Pancreatic Ductal Adenocarcinoma within Whipple Specimens, and Their Clinical Significance: Importance of Focused Lymph Node Examination, and Sampling of the Anterior Surfaces

Burcu Saka[1], Serdar Balci[2], Burcin Pehlivanoglu[3], Pelin Bagci[4], Bahar Memis[5], Michelle Reid[6], Olca Basturk[7], N. Volkan Adsay[8]

[1]Koç University School of Medicine, Istanbul, Turkey, [2]Independent Consultant, Turkey, [3]Dokuz Eylul University, Izmir, Turkey, [4]Marmara University, Istanbul, Turkey, [5]SBU Sisli Hamidiye Etfal Training and Research Hospital, Istanbul, Turkey, [6]Emory University Hospital, Atlanta, GA, [7]Memorial Sloan Kettering Cancer Center, New York, NY, [8]Koç University Hospital, Istanbul, Turkey

Disclosures: Burcu Saka: None; Serdar Balci: None; Burcin Pehlivanoglu: None; Pelin Bagci: None; Bahar Memis: None; Michelle Reid: None; Olca Basturk: None; N. Volkan Adsay: None

Background: Data regarding the spread patterns of pancreatic ductal adenocarcinoma (PDAC) within pancreatoduodenectomy specimens is highly limited. Especially, the involvement of different lymph node (LN) regions and their significance are not known.

Design: 192 consecutive Whipples for PDAC that were processed according to an established “orange peel”(PMID: 24451278) protocol that examines the lymph nodes along with the peripancreatic soft tissues in 7 regions were analyzed. Only ordinary PDACs were included.

Results: I. Metastasis to lymph nodes: LN mets was seen in 77% of PDACs. Posterior region lymph nodes were much more likely to be involved than the anterior (71% vs 41%) and median number of LNs involved was also higher in the posterior. Overall, uncinate/retroperitoneal region lymph nodes were the most common to be positive (35%), followed by those in posterior pancreatoduodenal groove (in 29%). Only a small percentage of the cases (6%) had LN mets in the anterior region only(without any LN positivity in the posterior aspect). While the presence of LN metastasis in the posterior region was associated with worse outcome (p=.00043), whether there was LN mets in the anterior region or not did not alter the outcome significantly. II. Invasion into peripancreatic soft tissue: Posterior soft tissues were more likely to be invaded by the carcinoma (80% vs 35%).The presence of invasion into anterior surfaces, which was often subtle, was associated with significantly worse outcome(p=.0015) and this was

independent of the size (stage) of the tumor in multivariate analysis with HR of 1.70 [CI:1.16-2.48;p=.006] for anterior soft tissue involvement, while it was HR of 1.02 [CI:1.00-1.03;p=.013] for tumor size.

Conclusions: Posterior aspect of the pancreas is more likely to contain LN metastasis and uncinate LNs are the ones that are most commonly positive. The presence of LN metastasis in the posterior is associated with worse outcome, whereas whether there is also LN mets in the anterior or not does appear to have any significant effect on prognosis. On the other hand, presence of carcinoma in the anterior soft tissues is an adverse prognostic factor. This study thus suggests that in PDACs that are seemingly LN negative (less than ¼ of the cases), special attention should be paid to posterior LNs, especially retroperitoneal, perhaps with additional scrutiny. It is also imperative that anterior soft tissue be examined carefully for subtle invasive carcinoma units because that alters the prognosis significantly.

1132 Ferroptosis in Extrahepatic Cholangiocarcinoma

Samantha Sarcognato[1], Diana Sacchi[1], Ivana Cataldo[1], Monia Niero[1], Giacomo Zanus[2], Maria Guido[2]
[1]Ospedale di Treviso, Treviso, Italy, [2]University of Padova, Padova, Italy

Disclosures: Samantha Sarcognato: None; Diana Sacchi: None; Ivana Cataldo: None; Monia Niero: None; Giacomo Zanus: None; Maria Guido: None

Background: Extrahepatic cholangiocarcinoma (eCCA) is an aggressive tumor with a poor prognosis, due to the absence of specific systemic treatments. A pro-inflammatory and anti-apoptotic microenvironment has been described in some eCCAs. Ferroptosis is a novel type of highly regulated iron-dependent cell death with a well known role in carcinogenesis. Triggering ferroptosis in cancer therapy is a promising option. Nothing is known about ferroptosis in eCCA. Therefore, the aim of this study was to investigate tissue expression of ferroptosis effectors in eCCA, and any correlation with prognostic and histological features.

Design: A series of 45 consecutive eCCA were enrolled and histologically reviewed; the main histological features were recorded. None of the patients received any neoadjuvant therapy before surgery. Immunostaining was performed on tissue microarrays, by using the following antibodies: TFR1 (Transferrin Receptor 1), GPX4 (the main ferroptosis inhibitor), STAT3 (as a marker of an anti-apoptotic milieu). Intracytoplasmic iron deposits were investigated by Perls' stain.

Results: A complete negativity for TFR1 was observed in 98%; none of the patients showed intracytoplasmic iron deposits in neoplastic cells. In 80% of cases GPX4 expression was absent. In 18% of cases a low GPX4 expression (<50% positive neoplastic cells) was found; however, there was no correlation with prognosis. A high STAT3 expression in neoplastic cells was observed in 51% of cases, and it was associated with a worse prognosis (reduced overall [p=0.001] and disease-free survival [trend, p=0.061], and unfavorable histological features (vascular invasion, p<0.001; perineural invasion, p=0.001).

Conclusions: Overexpression of STAT3 confirms an anti-apoptotic background in eCCA. However, ferroptosis does not seem activated in eCCA and it seems to be not inhibited by GPX4, which is absent in most cases. This highlights the possibility to use ferroptosis-inducer drugs in eCCA, such as Xc^- inhibitors and iron-overload drugs.

1133 Genomic Landscape of Clinically Advanced KRAS Wild-Type Pancreatic Ductal Adenocarcinoma (PDA)

Serenella Serinelli[1], Daniel Zaccarini[2], Vamsi Parimi[3], Richard Huang[4], Natalie Danziger[5], Tyler Janovitz[5], Jeffrey Ross[1]
[1]SUNY Upstate Medical University, Syracuse, NY, [2]SUNY Upstate Medical University, New York, NY, [3]Foundation Medicine, Inc., RTP, NC, [4]Foundation Medicine, Inc., Cary, NC, [5]Foundation Medicine, Inc., Cambridge, MA

Disclosures: Serenella Serinelli: None; Daniel Zaccarini: None; Vamsi Parimi: *Employee*, Foundation Medicine Inc.; Richard Huang: *Employee*, Foundation Medicine, Roche; Natalie Danziger: *Employee*, Foundation Medicine Inc.; *Stock Ownership*, F. Hoffman La Roche Ltd.; Tyler Janovitz: *Employee*, Foundation Medicine, Roche; Jeffrey Ross: *Employee*, Foundation Medicine

Background: Pancreatic ductal adenocarcinoma (PDA) is a lethal disease, with a 5-year survival rate <10%. The main genomic trait of PDA is *KRAS* oncogene mutation, which is seen in approximately 90% of cases. Many efforts have been made to target directly and indirectly the function of mutated KRAS oncoprotein, without significant survival improvements. *KRAS* wild-type PDA is a distinct molecular subtype of PDA, whose genomic hallmarks are represented by activated MAPK due to *BRAF* mutations, MSI,

and kinase-fusion genes. These PDAs can potentially be treated with *BRAF* antagonists, MAPK inhibitors, immunotherapy, and kinase inhibitors.

This study aims to compare the genomic features of *KRAS*-mutated and *KRAS* wild-type PDAs.

Design: Genomic alterations (GA) detected by a hybrid capture-based comprehensive genomic profiling assay were determined on 9,444 cases of clinically advanced PDA. Tumor mutational burden (TMB) was determined on 0.8-1.1 Mbp of sequenced DNA and microsatellite instability (MSI) was determined on 114 loci. PD-L1 expression in tumor cells (Dako 22C3) was measured by IHC.

Results: 721 (7.6%) PDAs were *KRAS* wild-type (*KRAS*wt) and 8,723 (92.4%) PDAs were *KRAS* mutated (*KRAS*m), Table 1. Ages were similar, KRASwt were more often male gender. GA/tumor were similar. For currently not targetable GA, *KRAS*wt featured greater frequencies of *ARID1A* and *RB1* GA and *KRAS*m featured greater frequencies in *TP53*, *CDKN2A/B*, *MTAP,* and *SMAD4*. With the exception of the *KRAS* G12C GA identified in 1.6% of the *KRASm* PDA, greater frequencies in currently potentially targetable genes were seen selectively among *KRASwt* including GA in *ERBB2* (amplifications and short variant GA), *BRAF*, *PIK3CA*, *FGFR1/2*, *PTEN*, and *ATM*. Although frequencies were low, the *KRAS*wt PDA featured greater frequencies of biomarkers associated with immune checkpoint inhibitor efficacy (IPCI) including *PBRM1* GA and TMB > 10 mutations/Mb although *KRAS*m PDA had a higher frequency of PD-L1 low but not high IHC expression.

Table 1. Overview of the genomic landscapes of *KRAS* mutated and *KRAS* wild-type PDAs.

	***KRAS* Wild-type**	***KRAS* Mutated**	**P Value**
Cases	721	8,723	
Males/Females	61%/39%	52%/48%	<.0001
Median age (range)	65 (22-89+)	67 (24-89+)	NS
Mean age	63.7	65.9	<.0001
GA/tumor	4.47	4.88	NS
Top Untargetable GA			
TP53	47.6%	80.2%	<.0001
CDKN2A	34.4%	56.2%	<.0001
CDKN2B	23.0%	28.9%	=.0007
SMAD4	15.7%	26.8%	<.0001
MTAP	18.0%	21.7%	=.02
CDK6	1.9%	2.7%	NS
ARID1A	13.6%	7.7%	<.0001
RB1	4.0%	2.0%	=.001
Top Potentially Targetable GA			
EGFR SV	<1%	<1%	NS
ERBB2 Amplification + SV	6.8%	1.7%	<.001
ALK Fusion	1.0%	0%	NS
BRAF	17.9%	0.5%	<.0001
PIK3CA	6.5%	2.3%	<.0001
FGFR1	1.2%	1.6%	NS
FGFR2	4.4%	0.1%	<.0001
PTEN	7.2%	1.2%	<.0001
KRAS G12C	0%	1.6%	<.0001
BRCA1	1.8%	1.2%	NS
ATM	6.8%	3.6%	<0001
BRCA2	2.5%	2.9%	NS
IO Predictive GA			
PBRM1	3.2%	0.7%	<.0001
STK11	3.3%	2.5%	NS
MDM2	4.4%	1.3%	<.0001
CD274 amplification	<1%	<1%	NS
IO Predictive Biomarkers			
MSI-High	1.7%	<0.9%	NS
Mean TMB	3.6	2.3	<.0001
Median TMB	2.5	1.3	
TMB>10 mut/Mb	6.3%	1%	<.0001
TMB>20 mut/Mb	2.4%	<0.5%	<.0001
PD-L1 IHC Low Positive	21.8% (257 cases)	31.8% (3069 cases)	=.0007
PD-L1 IHC High Positive	6.0%	5.7%	NS

Conclusions: Therapeutic management of PDA remains an important challenge. Our results confirm those reported in the literature, according to which many targetable genes and a high TMB are significantly more common among *KRAS* wild-type PDAs. Moreover, classification of PDAs into *KRAS* mutated vs KRAS wild-type categories may be clinically beneficial in summarizing the genomic profile and the available targeted therapies. Our findings highlight the importance of comprehensive genomic analysis to find molecular targets including gene fusions for precision oncology.

1134 Cancer Cells with Stem-Like and Epithelial-Mesenchymal Transition Properties Are Uniformly Present in Pancreatic Ductal Adenocarcinoma and Persist After Neoadjuvant Therapy

Hania Shakeri[1], Kevin Kuan[1], Nicole Panarelli[2]
[1]Albert Einstein College of Medicine, Montefiore Medical Center, Bronx, NY, [2]Montefiore Medical Center - Moses Division, Bronx, NY

Disclosures: Hania Shakeri: None; Kevin Kuan: None; Nicole Panarelli: None

Background: Overwhelming metastatic burden in pancreatic ductal adenocarcinoma (PDAC) is driven by cancer cells with stem-like and mesenchymal properties and contributes to its almost uniformly fatal outcome. Cancer stem cell (CSC) markers, ALDH1 and PROM1, are up-regulated in multiple tumor types, whereas e-cadherin is reduced, signifying epithelial-mesenchymal transition (EMT). We performed this pilot study to evaluate the expression of these markers in treatment naïve and neoadjuvantly treated PDAC and to correlate their expression with pathologic features.

Design: We retrospectively identified patients (Male: female = 2:3; mean age: 72 years) who had undergone curative intent resection for PDAC with (n=18) or without (n=12) neoadjuvant therapy. Tumor grade and tumor regression grade (TRG) were assigned according the College of American Pathologists criteria. Moderate or strong cytoplasmic staining in ≥25% and membranous or cytoplasmic staining of greater intensity than non-neoplastic ducts in tumor cells was considered overexpression for ALDH1 and PROM1, respectively. Weak, discontinuous membranous reactivity in ≥25% of tumor cells denoted e-cadherin loss. Fisher's exact test was used to compare staining patterns among groups.

Results: Most PDACs showed abnormal expression of ALDH1 (24/30, 80%), whereas PROM1 was overexpressed in 17/30 (56%) cases and in all high-grade tumors. E-cadherin expression was also abnormal in most cases (25/30, 83%) and in all high-grade tumors (Table). Abnormal PROM1 and e-cadherin were significantly correlated with high tumor grade ($p<0.0001$ and 0.05, respectively). All tumors showed aberrant expression of at least one marker, and 26/30 (87%) aberrantly expressed at least 2 of these markers. Aberrant expression was evenly distributed among treatment naïve vs. neoadjuvantly treated, lymph node positive vs. lymph node negative cases, and TRGs with no statistically significant differences observed (Figure).

Tumor Feature	ALDH1	PROM1	E-cadherin
Treatment naïve (n=12)	10, 83%	8, 67%	11, 92%
Neoadjuvant (n=18)	14, 78%	9, 50%	14, 78%
TRG1 (n=7)	6, 86%	4, 57%	6, 86%
TRG2-3 (n=11)	8, 73%	5, 45%	8, 73%
Low-grade (n=17)	13, 76%	4, 24%	12, 71%
High-grade (n=13)	11, 85%	13, 100%	13, 100%
No lymph node metastases (n=14)	11, 79%	6, 43%	10, 71%
Lymph node metastases (n=16)	13, 81%	11, 69%	15, 94%

Figure 1 - 1134

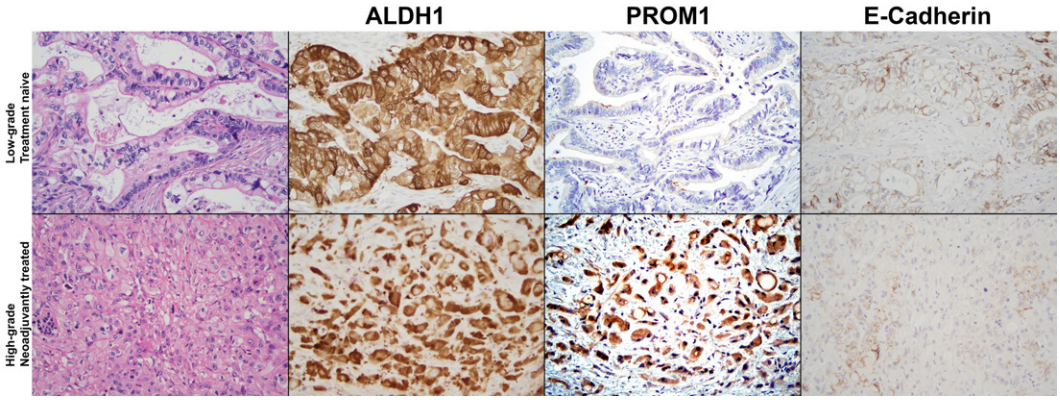

Conclusions: Stem-like and EMT properties are intrinsic to PDAC regardless of grade, and all high-grade tumors exhibit aberrant PROM1 and e-cadherin, both described as poor prognostic indicators in other malignancies. These features likely contribute to uniformly aggressive behavior despite tumor stage, grade, or TRG. Additional studies may support their value as a prognostic tool. Their presence in treatment naïve and neoadjuvantly treated tumors underscores the inadequacies of current therapeutic regimens, which fail to eradicate these populations.

1135 A Prospective Multi-Institutional Study Reveals the Combination of Next-Generation Sequencing and Cytology Improved the Evaluation of Pancreatic Cyst Patients

Aatur Singhi[1], Abigail Wald[1], Sigfred Lajara[2], N. Paul Ohori[3], Marina Nikiforova[1]
[1]University of Pittsburgh Medical Center, Pittsburgh, PA, [2]University of Pittsburgh Medical Center Presbyterian Shadyside, Pittsburgh, PA, [3]UPMC Presbyterian Hospital, Pittsburgh, PA

Disclosures: Aatur Singhi: *Consultant*, Foundation Medicine; Abigail Wald: None; Sigfred Lajara: None; N. Paul Ohori: None; Marina Nikiforova: *Stock Ownership*, University of Pittsburgh; *Consultant*, Sonic Healthcare USA

Background: Next-generation sequencing (NGS) of pancreatic cyst fluid (PCF) is a useful adjunct to the evaluation of pancreatic cyst patients. For instance, MAPK/*GNAS* mutations are specific for mucinous cysts, while alterations in *TP53*, *SMAD4*, *CTNNB1,* and the mTOR genes are associated with advanced neoplasia (high-grade dysplasia and adenocarcinoma). However, previous studies have been retrospective or a single institutional experience. The aim of this study was to prospectively evaluate the accuracy of NGS testing in the detection of mucinous cysts and advanced neoplasia across multiple institutions.

Design: Within 24 months, EUS-FNA obtained PCF was received from 31 institutions and in real-time subjected to NGS of 22 genes (PancreaSeq). Targeted NGS data to include allele frequency (AF) was correlated with fluid viscosity, CEA, clinical presentation, imaging findings, cytology, and follow-up data.

Results: Among 1933 PCF specimens, 1887 (98%) from 1832 patients were satisfactory for NGS. Genomic alterations were found in 1220 (65%) cysts and 1049 (56%) cases harbored alterations in the MAPK/*GNAS* genes. Further, 169 of 1049 (16%) MAPK/*GNAS*-mutant cysts had *TP53*, *SMAD4*, *CTNNB1*, and/or mTOR gene mutations. Low-level AF mutations in *TP53*, *CTNNB1*, and *PIK3CA* were seen in 31 (18%) cases. Follow-up was available for 1216 of 1832 (66%) patients with a median of 23 months. Based on 251 (21%) patients with diagnostic surgical pathology, MAPK/*GNAS* mutations had a 90% sensitivity and 100% specificity for a mucinous cyst. In comparison, fluid viscosity and elevated CEA had lower sensitivities (77% and 73%) and lower specificities (92% and 94%). In combination with MAPK/*GNAS* mutation, alterations in *TP53*, *SMAD4*, *CTNNB1*, and/or the mTOR genes had 88% sensitivity and 95% specificity for a mucinous cyst with advanced neoplasia. Exclusion of low-level *TP53*, *CTNNB1*, and *PIK3CA* mutations, improved the specificity to 98%. Worrisome clinical and imaging findings, and cytology of at least suspicious for adenocarcinoma had lower diagnostic performance. However, combining NGS testing and cytology improved the sensitivity of advanced neoplasia to 93%, while maintaining a high specificity of 95%. Of the remaining 965 patients, none reported a diagnosis of malignancy.

Conclusions: Prospective NGS was superior to other modalities in the detection of mucinous cysts and advanced neoplasia. However, the sensitivity of NGS testing for advanced neoplasia improved when used in combination with cytologic evaluation.

1136 Integrated Pathologic Score Effectively Stratifies Patients with Pancreatic Ductal Adenocarcinoma Who Received Neoadjuvant therapy and Pancreaticoduodenectomy

Aaron Sohn[1], Matthew Katz[1], Laura Prakash[1], Deyali Chatterjee[1], Hua Wang[1], Michael Kim[1], Ching-Wei Tzeng[1], Jeffrey Lee[1], Naruhiko Ikoma[1], Asif Rashid[1], Robert A. Wolff[1], Dan Zhao[1], Eugene Koay[1], Anirban Maitra[1], Huamin Wang[1]
[1]The University of Texas MD Anderson Cancer Center, Houston, TX

Disclosures: Aaron Sohn: None; Matthew Katz: None; Laura Prakash: None; Deyali Chatterjee: None; Hua Wang: None; Michael Kim: None; Ching-Wei Tzeng: *Consultant*, PanTher Therapeutics; Jeffrey Lee: None; Naruhiko Ikoma: None; Asif Rashid: None; Robert A. Wolff: None; Dan Zhao: None; Eugene Koay: None; Anirban Maitra: *Primary Investigator*, Cosmos Wisdom Biotechnology, Thrive Earlier Detection (an Exact Sciences Company); *Consultant*, Freenome, Tezcat Biotech; Huamin Wang: None

Background: Neoadjuvant therapy (NAT) is increasingly used to treat patients with pancreatic ductal adenocarcinoma (PDAC). Pathologic parameters of treated PDAC, including tumor (ypT) and lymph node (ypN) stage, and tumor response grading are important prognostic factors in this group of patients. Currently the integrated pathologic score (IPS) that combines ypT, ypN, and tumor response grading in treated PDAC patients has not been reported.

Design: Our study group consisted of 398 PDAC patients who received NAT and underwent pancreaticoduodenectomy (PD) at our institution (222 males and 176 females with a median age of 64.1 years). All PD specimens were evaluated using a standardized protocol. The IPS was calculated as the sum of the scores for ypT (0, ypT0; 1, ypT1; 2, ypT2; and 3, ypT3), ypN (0, ypN0; 1, ypN1; and 2, ypN2), and tumor response grading according to either MD Anderson grading system (IPSMDA) or CAP grading system (IPSCAP). The IPSMDA, IPSCAP and AJCC stages (8^{th} edition) were correlated with patient survival using Kaplan-Meier or Cox Regression analysis.

Results: Using either IPSMDA or IPSCAP, PDAC patients were stratified into four distinct prognostic groups for both disease-free survival (P<0.001) and overall survival (P<0.001): Group 1, IPSMDA of 0-1 or IPSCAP of 0-1; Group 2, IPSMDA of 2-3 or IPSCAP of 2-3; Group 3, IPSMDA of 4-5 or IPSCAP of 4-6; and Group 4, IPSMDA of 6-7 or IPSCAP of 7-8. In multivariate analysis, IPSMDA, IPSCAP and AJCC stage were independent prognostic factor for both disease-free survival (DFS) (P<0.001) and overall survival (OS) (P<0.001). However, patients with AJCC stage IB, IIA or IIB disease had no significant difference in either DFS or OS (P>0.05).

Mean DFS and OS for IPSMDA and IPSCAP

	IPSMDA	**IPSMDA**	**IPSCAP**	**IPSCAP**
	DFS (months)	OS (months)	DFS (months)	OS (months)
Group 1	148.2 ± 21.7	159.1 ± 18.6	148.2 ± 21.7	159.1 ± 18.6
Group 2	101.0 ± 11.4	123.7 ± 10.9	98.1 ± 12.5	122.6 ± 12.0
Group 3	58.0 ± 6.1	73.0 ± 5.7	57.8 ± 5.6	73.6 ± 5.2
Group 4	17.1 ± 3.1	35.4 ± 3.4	13.0 ± 2.7	28.3 ± 3.8
p-value	<0.001	<0.001	<0.001	<0.001

Conclusions: Both IPSMDA and IPSCAP effectively stratify treated PDAC patients into four distinct prognostic groups and are independent prognosticators for both disease-free survival and overall survival. The IPS can be used a new prognostic marker for treated PDAC patients. Our data also suggest that a different AJCC stage grouping for treated PDAC patients with stage IB, IIA, and IIB disease.

1137 A Single Center Clinicopathological Study of Comparison of Pancreatic Acinar Cell Carcinoma and its Mixed Differentiations

Lei Sun[1], Aaron Sohn[1], Matthew Katz[1], Laura Prakash[1], Hua Wang[1], Michael Kim[1], Ching-Wei Tzeng[1], Jeffrey Lee[1], Naruhiko Ikoma[1], Asif Rashid[1], Robert A. Wolff[1], Dan Zhao[1], Eugene Koay[1], Anirban Maitra[1], Huamin Wang[1]
[1]The University of Texas MD Anderson Cancer Center, Houston, TX

Disclosures: Lei Sun: None; Aaron Sohn: None; Matthew Katz: None; Laura Prakash: None; Hua Wang: None; Michael Kim: None; Ching-Wei Tzeng: *Consultant*, PanTher Therapeutics; Jeffrey Lee: None; Naruhiko Ikoma: None; Asif Rashid: None; Robert A. Wolff: None; Dan Zhao: None; Eugene Koay: None; Anirban Maitra: *Primary Investigator*, Cosmos Wisdom Biotechnology, Thrive Earlier Detection (an Exact Sciences Company); *Consultant*, Freenome, Tezcat Biotech; Huamin Wang: None

Background: Pancreatic acinar cell carcinoma (ACC) and mixed ACC are rare malignant epithelial neoplasms. The survival for patients with ACC is poor with a reported median survival of 19 months. A mixed acinar cell carcinoma subtypes with neuroendocrine, ductal, or both differentiation can be seen. Due to the rarity of these tumors, the clinicopathological features, particularly for mixed ACC subtypes, remain unclear. The purpose of this study is to examine the clinicopathological features and survival of ACC and mixed ACC subtypes, including mixed acinar- neuroendocrine carcinoma (MANEC), acinar- ductal carcinoma (MADC), and mixed acinar- neuroendocrine- ductal carcinoma (MANDC).

Design: Our study group consisted of 55 cases who underwent resection at our institution and included 34 ACCs, 11 MANECs, 8 MADCs, and 2 MANDCs. The diagnosis for all cases was reviewed and confirmed based on the WHO classification. The clinicopathologic information was obtained from patient medical records. For statistical analysis, 2 MANDCs were combined as the MANEC group. Survival analyses were performed using the Kaplan-Meier method and the correlations of various parameters were analyzed using the Chi-Square analysis. Statistical significance was considered if the P-value was <0.05.

Results: The age of all patients ranged from 24 to 81 years (median: 58 years). The M: F ratio is 2:1. The tumor size ranges from 0.6 cm to 20.0 cm (median: 4.0 cm). MADCs occurred more frequently in the pancreatic head (87.5%), compared with pure ACCs (45.5%) and MANEC group (46.2%). Lymph node metastasis was present in 38.5%, 100%, and 53.8% of ACCs, MADCs, and MANEC group respectively ($p<0.001$). At time of surgery, distant metastasis was present in 14.7% of ACCs, 0% of MADCs, and 23.1% of MANEC group ($p = 0.35$). The median overall survival for MANEC group is 17.0 (95% CI: 1.0-33.0) months, which was significantly shorter than ACCs (52.9 months, 95% CI: 24.5-81.3 months) and MADCs (33.8 months, 95% CI: 11.8-55.8 months ($p = 0.009$). There was no significant difference in survival between ACCs and MADCs ($p > 0.05$). There were no significant differences in other clinicopathologic parameters among ACCs, MADCs, and MANEC group ($p > 0.05$).

Conclusions: The MANEC group has a much shorter overall survival compared with pure ACCs and MADCs. MADCs have a higher frequency of lymph node metastasis than ACCs and the MANEC group.

1138 Blinded Histologic Review to Classify Grade 3 Pancreatic Epithelial Neuroendocrine Neoplasms Shows Only Slight Correlation Among Experienced Gastrointestinal Pathologists

Mehran Taherian[1], Rebecca Waters[1], Wai Chin Foo[1], Dipen Maru[1], Susan Abraham[1], Asif Rashid[1], Huamin Wang[1], Dongguang Wei[1], Melissa Taggart[1], Deyali Chatterjee[1]
[1]The University of Texas MD Anderson Cancer Center, Houston, TX

Disclosures: Mehran Taherian: None; Rebecca Waters: *Advisory Board Member*, Astellas; *Advisory Board Member*, Astellas; Wai Chin Foo: None; Dipen Maru: None; Susan Abraham: None; Asif Rashid: None; Huamin Wang: None; Dongguang Wei: None; Melissa Taggart: None; Deyali Chatterjee: None

Background: The pathogenesis, biologic behavior, and treatment of well-differentiated neuroendocrine tumors (NET) and poorly differentiated neuroendocrine carcinomas (NEC) are different. The diagnosis relies on multiple factors, but pathologic assessment is crucial. Based on currently available diagnostic criteria, the distinction between NET G3 and NEC are made on morphologic assessment, without taking Ki-67 proliferative index into consideration. This study looks at the concordance rates among experienced gastrointestinal pathologists following published guidelines (current WHO criteria and additional morphologic criteria based on a recent international consensus study) and how it compares to clinical parameter-based retrospective categorization.

Design: 32 cases of NET G3 and NEC were selected from a retrospective search of cases for pancreatic neuroendocrine neoplasms, with tumor slide availability in-house, including Ki-67 stain. A morphologic review was performed by 8 GI pathologists (blinded to all other information, including proliferative indices), practicing at a tertiary cancer center for a median of 20 years. A

clinical diagnosis was separately formulated based on information collected from electronic medical records focusing on special imaging results (octreotide/ gallium scan, FDG-PET), molecular data (if available), and clinical course of the disease, including survival and response to treatment received. Reliability assessment and correlations were studied using standard statistical software.

Results: The interobserver agreement results on the diagnosis, as well as individual histologic parameters assessed by all pathologists are highlighted in Table 1. The "gold standard" diagnosis formulated based on multiple clinical parameters correlated strongly with overall survival (2071+/- 13 days for NET and 720 +/- 386 days for NEC; p=0.006) as well as Ki-67 proliferative index (33 +/- 17 for NET and 53 +/- 22 for NEC; p=0.01). Ki-67 proliferative index also independently showed negative correlation with survival (p=0.027).

Parameter	Kappa value (interobserver agreement)
Consensus on diagnosis of NET-G3 and NEC	0.329 (slight)
Consensus on not calling a small cell carcinoma	0.908 (almost perfect)
Consensus on individual diagnostic parameters*	
Architecture	0.245 (slight)
Vascular pattern	0.139 (no)
Desmoplastic stroma	0.244 (slight)
Absence of necrosis	0.851 (almost perfect)

* Elvebakken H, et al. A Consensus-Developed Morphological Re-Evaluation of 196 High-Grade Gastroenteropancreatic Neuroendocrine Neoplasms and Its Clinical Correlations. Neuroendocrinology. 2021;111(9):883-894.

Figure 1 - 1138

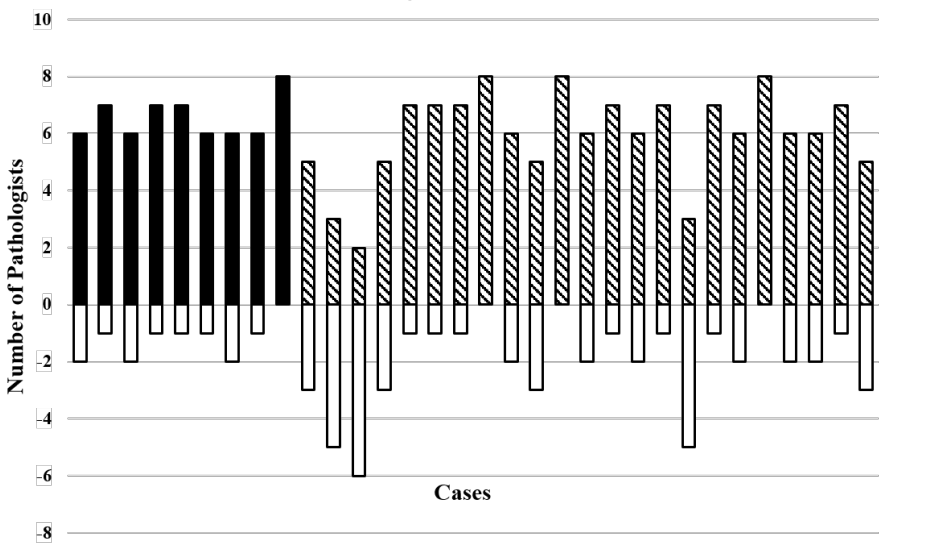

Conclusions: The distinction between NET G3 and NEC solely based on morphology, as is the current recommendation, is challenging, especially in a small biopsy. Ancillary studies (immunohistochemistry and/or molecular studies) and correlation with clinical datapoints such as special imaging (octreotide, 68-Gallium DOTATATE, and/or FDG PET), clinical course and tumor response to therapy is probably warranted.

1139 Pathologic Prognosticators for Patients with Pancreatic Ductal Adenocarcinoma Who Received Neoadjuvant FOLFIRINOX or Gemcitabine/Nab-Paclitaxel Therapy

Yi Tat Tong[1], Zongshan Lai[1], Matthew Katz[1], Laura Prakash[1], Hua Wang[1], Deyali Chatterjee[1], Michael Kim[1], Ching-Wei Tzeng[1], Jeffrey Lee[1], Naruhiko Ikoma[1], Asif Rashid[1], Robert A. Wolff[1], Dan Zhao[1], Eugene Koay[1], Anirban Maitra[1], Huamin Wang[1]
[1]The University of Texas MD Anderson Cancer Center, Houston, TX

Disclosures: Yi Tat Tong: None; Zongshan Lai: None; Matthew Katz: None; Laura Prakash: None; Hua Wang: None; Deyali Chatterjee: None; Michael Kim: None; Ching-Wei Tzeng: *Consultant*, PanTher Therapeutics; Jeffrey Lee: None; Naruhiko Ikoma: None; Asif Rashid: None; Robert A. Wolff: None; Dan Zhao: None; Eugene Koay: None; Anirban Maitra: *Primary Investigator*, Cosmos Wisdom Biotechnology, Thrive Earlier Detection (an Exact Sciences Company); *Consultant*, Freenome, Tezcat Biotech; Huamin Wang: None

Background: Neoadjuvant FOLFIRINOX or gemcitabine/nab-paclitaxel therapy are increasingly used in patients with pancreatic ductal adenocarcinoma (PDAC). However, the pathologic prognostic factors in post-treatment pancreatectomy specimens from this group of patients remain unclear. The purpose of this study is to systematically evaluate the pathologic parameters and to correlate with disease-free survival (DFS) and overall survival (OS).

Design: This study consisted of 284 consecutive PDAC patients who received FOLFIRINOX (213 patients) or gemcitabine /nab-paclitaxel (71 patients) with radiation and pancreatectomy at our institution. The clinical and pathologic information were retrieved from a prospectively maintained database and verified by reviewing patients' medical records. Correlations of clinicopathologic parameters with survival were analyzed by univariate and multivariate Cox regression. Chi-square tests were used to compare categorical data between two groups.

Results: Among the 284 patients, 12 (4.2%), 29 (10.2%), and 243 (85.6%) patients had MD Anderson grade 0, 1, and 2 response, respectively, and 12 (4.2%), 29 (10.2%), 140 (49.3%), and 103 (36.3%) had CAP grade 0, 1, 2 and 3 response, respectively. The MD Anderson grading correlated with both DFS ($p = 0.001$) and OS ($p = 0.001$). However, there was no significant difference in either DFS or OS between CAP grade 2 and grade 3 ($p > 0.05$). In addition, the ypN and ypT stages correlated with both DFS and OS. Similar to our previous study, we found that ypT0/1a/1b had better OS than those with ypT1c ($p = 0.045$), but there were no significant differences in either DFS or OS between ypT1c and ypT2 ($p >0.05$). In multivariate analysis, MD Anderson grading and ypN were independent prognostic factors for DFS ($p=0.002$ and $p=0.01$, respectively) and MD Anderson grading was an independent prognostic factor for OS ($p=0.006$).

Conclusions: Our study demonstrates that the MD Anderson grading system correlates with and is an independent prognostic factor for both DFS and OS. There is no significant difference in either DFS or OS between CAP grade 2 and 3. The ypT and ypN are also important prognostic factors in this group of treated PDAC patients. In addition, our study suggests that 1.0 cm is a better cut off for ypT2 stage.

1140 Diagnostic Utility of Somatostatin Receptor Subtype 2A in Distinguishing Pancreatic NET from NEC

Sarah Umetsu[1], Olca Basturk[2], Deyali Chatterjee[3], Gillian Hale[4], Nafis Shafizadeh[5], Grace Kim[1], Sanjay Kakar[1], Nancy Joseph[1]
[1]University of California, San Francisco, San Francisco, CA, [2]Memorial Sloan Kettering Cancer Center, New York, NY, [3]The University of Texas MD Anderson Cancer Center, Houston, TX, [4]The University of Utah, Salt Lake City, UT, [5]Kaiser Permanente, Woodland Hills, CA

Disclosures: Sarah Umetsu: None; Olca Basturk: None; Deyali Chatterjee: None; Gillian Hale: None; Nafis Shafizadeh: None; Grace Kim: None; Sanjay Kakar: None; Nancy Joseph: None

Background: Well-differentiated neuroendocrine tumors (NET) and neuroendocrine carcinoma (NEC) both share expression of neuroendocrine markers (synaptophysin, chromogranin), but are biologically distinct entities with different clinical behaviors and treatments. Grade 3 NET and NEC are both defined by Ki67>20% and/or mitoses >20 per $2mm^2$ and can be challenging to distinguish based on morphology alone. The majority of NET express high levels of somatostatin receptor subtype 2A (SSTR2A), which is the basis of therapy with the somatostatin analogue octreotide, whereas NEC typically show negative to patchy weak expression. Because of these differences, SSTR2A has been suggested as a useful diagnostic tool in differentiating G3 NET from NEC (PMID 31857137). This study examines the role of SSTR2A in this distinction.

Design: SSTR2A IHC (clone UMB1, Abcam) staining intensity (weak, variable, strong) and extent of staining (0-5%, 5-20%, 21-50%, 51-90%, >90%) were evaluated on 30 pancreatic NET and 22 pancreatic NEC. All cases were classified using H&E, synaptophysin, chromogranin, trypsin, Ki-67, and molecular profiling using a capture based next-generation sequencing assay of 479 cancer genes.

Results: 27/30 (90%) NET showed diffuse SSTR2A staining in >90% of tumor cells, while only 6/22 (27%) NEC showed diffuse staining in >90% of cells ($p<0.0001$). In contrast, only 1 NET (3%) showed <5% positivity, while 10/22 (45%) NEC showed <5% staining ($p<0.0003$). When NET were subdivided by grade (G1-G2 verus G3), 19/20 (95%) of G1-G2 NET showed strong diffuse SSTR2A staining in >90% of cells, whereas only 3/10 (30%) G3 NET showed strong diffuse staining in >90% of cells, and 5/10 (50%) showed variable diffuse staining in >90% of cells. Furthermore, 2/10 (20%) of G3 NET had less than 50% staining, whereas only 5% of G1-G2 NET had less than 50% staining. All types of NEC showed a range in the extent and intensity of staining. Notably, all groups of NEC had some cases with strong diffuse staining in >90% of cells, as well as cases with staining in <5% of cells.

Table 1a. SSTR2A staining patterns in pancreatic NET versus NEC

Extent of SSTR2A staining	All NET (n=30)	All NEC (n=22)	P value
>90%	27 (90%) 22 strong, 5 variable	6 (27%) 5 strong, 1 variable	<0.0001
51-90%	0	0	---
21-50%	1 (3%) strong	2 (9%) 1 weak, 1 variable	0.567
5-20%	1 (3%) weak	4 (18%) 3 strong, 1 weak	0.1494
<5%	1 (3%)	10 (45%)	<0.0003

Table 1b SSTR2A staining patterns in NET and NEC separated by grade and subtype respectively

Extent of SSTR2A staining	G1/G2 NET (n=20)	G3 NET (n=10)	Pure NEC (8)	Mixed adeno/NEC (6)	Mixed ACC/NEC (8)
>90%	19 (95%) All strong	8 (80%) 3 strong, 5 variable	4 (50%) 3 strong, 1 variable	1 (17%) strong	1 (13%) strong
51-90%	0	0	0	0	0
21-50%	0	1 (10%) strong	0	2 (33%) 1 variable, 1 weak	0
5-20%	0	1 (10%) weak	2 (25%) 1 strong, 1 weak	0	2 (25%) strong
<5%	1 (5%)	0	2 (25%)	3 (50%)	5 (63%)

Conclusions: The vast majority (95%) of G1-G2 NET show strong diffuse staining for SSTR2A. In contrast, G3 NETs often show diffuse staining (80%), but with more variable intensity and 20% of G3 NET show less than 50% staining. In NEC, SSTR2A staining can be diffuse and strongly positive in ~25% of cases; thus, a strong diffuse SSTR2A does not exclude a diagnosis of NEC. However, almost 50% of NEC are SSTR2A-negative, whereas only 3% of NET are SSTR2A-negative; thus, negative SSTR2A can be useful in further confirming a diagnosis of NEC.

1141 BLM, MYH9, and PCK1 Mutations are Possible Markers of Metastatic Potential in Pancreatic Solid Pseudopapillary Tumors

Benjamin VanTreeck[1], Hee Eun Lee[1], Colton McNinch[1], Lizhi Zhang[1]
[1]*Mayo Clinic, Rochester, MN*

Disclosures: Benjamin VanTreeck: None; Hee Eun Lee: None; Colton McNinch: None; Lizhi Zhang: None

Background: Pancreatic solid pseudopapillary tumor (PSPT) is a low-grade malignant neoplasm that most frequently affects young women. Mutations of *CTNNB1* lead to activation of APC/β-catenin pathway; however, little is known regarding genetic events that are associated with PSPT metastatic progression. In this study, we used RNA sequencing to elucidate potential genetic markers or indicators of metastatic potential in PSPT.

Design: Transcriptome sequencing on formalin-fixed paraffin-embedded tissue of resected non-metastatic PSPTs (n=6) and metastatic PSPTs (n=3) without paired primary tumor, along with corresponding paired normal tissue was performed. Sequencing reads were aligned using STAR against the HG38 reference genome, using the ENSEMBL reference release 78, and variants were subsequently called with GATK HaplotypeCaller. Mutations in *CTNNB1* and all mutated genes exclusively shared by the 3 cases of metastatic PSPT were identified and analyzed.

Results: Clinicopathologic data for the 9 PSPT cases is summarized in Table 1. RNA sequencing revealed no significant gene fusions identified in all PSPT cases. All cases of PSPT demonstrated biallelic *CTNNB1* missense mutations in exon 3. Variant analysis of all cases showed 101 gene mutations exclusively shared by metastatic PSPT that were not identified in nonmetastatic PSPT. Of the 101 genes, the following 3 genes may potentially act as tumor suppressors and participate in metastatic progression: *BLM*, *MYH9*, and *PCK1*. Each case of metastatic PSPT demonstrated one or more biallelic mutations in each of the previously mentioned genes leading to missense, frameshift, stop gained, splice donor, splice acceptor, or splice region protein alterations.

A single mutation in *MYH9* (c.5797C>T) is the only confirmed pathogenic mutation based on a review in GeneReviews/OMIM databases. Two addition mutations, *BLM* (c.377C>T) and *PCK1* (c.228G>T), each have an uncertain significance in INVITAE and Illumina databases, respectively. The remaining mutations have an unknown pathogenic potential.

Figure 1 - 1141

Table 1. Clinicopathologic Characteristics

	Non-metastatic PSPT (n=6)	Metastatic PSPT (n=3)
Age, median (range)	38 (22-64)	48 (24-52)
Sex (F,M)	5,1	3,0
Primary Tumor Size (cm), median (range)	7.2 (2.1-12.2)	N/A
Location	Pancreas	Liver

Abbreviations: PSPT, pancreatic solid pseudopapillary tumor; F, female; M, male

Conclusions: We demonstrated that all non-metastatic and metastatic PSPT in our cohort contain a *CTNNB1* missense mutation in exon 3. Furthermore, we identified 3 genes only mutated in metastatic PSPT, *BLM*, *MYH9*, and *PCK1*, that may potentially participate in PSPT metastatic progression. Additional investigation is required to determine if these 3 genes play a significant role in PSPT metastatic progression and are definitively associated with metastatic potential.

1142 HNF4α Promoter 1 Isoforms, not Promoter 2 Isoforms, are Correlated with Dysplasia in Intraductal Papillary Mucinous Neoplasms

Jahg Wong[1], Vincent Quoc-Huy Trinh[2], Marcus Tan[2]
[1]Centre Hospitalier de l'Université de Montréal (CHUM), Montreal, Canada, [2]Vanderbilt University Medical Center, Nashville, TN

Disclosures: Jahg Wong: None; Vincent Quoc-Huy Trinh: None; Marcus Tan: None

Background: Hepatocyte nuclear factor 4 alpha (HNF4α) has been described as a master regulator of differentiation in the liver and some foregut organs. Alternative splicing yields isoforms are grouped into promoters P1 and P2 which have distinct roles in various organs and cancers, notably P1 is associated with metabolism while P2 is associated with proliferation. Our goal was to test for differential roles of HNF4α isoforms in IPMNs.

Design: R&DSystems have developed P1 isoforms (R&D Systems PP-K9218-00) and P2 isoforms (R&D PP-H6939-00) specific antibodies for human samples which were stained in 29 patient IPMNs from our institutional cohort. Expression pattern and localization was scored by two pathologists of the percentage of positive nuclear and cytoplasmic staining. Discordances were resolved after review. Nuclear and cytoplasmic staining patterns were given a score of 0 (0 to 50% mild), 1 (50% mild to 50% moderate), 2 (50% moderate to 50% strong), and 3 (50% strong to 100% strong. Statistics were performed in PRISM GraphPad v8 and SPSS v26.

Results: 15 LG and 14 HG IPMNs were included. P1 is differentially expressed in IPMNs, with lower grade components showing patchy heterogenous expression, while being diffusely expressed in higher grade components within the same IPMN (figure 1). P2 was expressed ubiquitously at stable levels throughout. Significantly higher nuclear expression and a trending lower cytoplasmic expression in high-grade IPMNs was noted for the P1 isoforms (figure 2). No trend was seen with the P2 isoforms.

Figure 1 - 1142

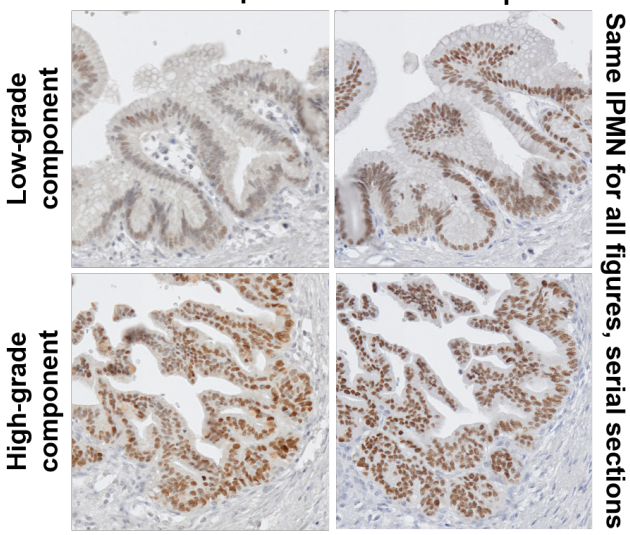

Figure 2 - 1142

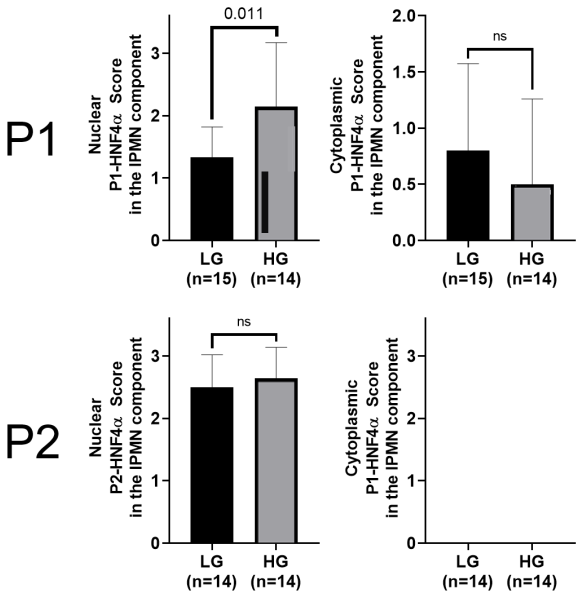

Conclusions: These findings suggest a correlation between P1-HNF4α isoforms and dysplastic progression in IPMNs, while P2 isoforms remained stable between LG and HG IPMNs. A possible cytoplasmic to nuclear shift is also noted. Further validation in a larger cohort, as well as identification of the specific P1 isoform, is warranted and under way in different models.

1143 Characterization of Insulin-Like Growth Factor II mRNA Binding Protein 3 Immunohistochemical Staining Patterns in Gallbladder Lesions

Limin Yang[1], Kara Phelps[2], Suntrea Hammer[3], Purva Gopal[3], James Mitchell[3]
[1]University of Texas Southwestern Medical Center, Dallas, [2]Incyte Diagnostics, Spokane Valley, WA, [3]UT Southwestern Medical Center, Dallas, TX

Disclosures: Limin Yang: None; Kara Phelps: None; Suntrea Hammer: None; Purva Gopal: None; James Mitchell: None

Background: Gallbladder carcinomas arise via a multistep carcinogenesis process, which may be related to chronic inflammation of the mucosal epithelium. The distinction between benign reactive epithelial atypia, low-grade dysplasia, and high-grade dysplasia can be histologically challenging. Expression of insulin-like growth factor II mRNA binding protein 3 (IMP3), a fetal oncoprotein that has been implicated in carcinogenesis, has been suggested to be a marker for high-grade dysplasia in the biliary tract; however, the staining pattern has not been well-characterized in low-grade dysplasia and reactive mucosal changes, particularly in the gallbladder.

Design: The aim of this study is to characterize the IMP3 immunohistochemical staining patterns of gallbladder lesions, to include reactive atypia, low-grade dysplasia, high-grade dysplasia, and invasive carcinoma from resection specimens. H&E-stained slides were screened by one pathologist to select representative blocks of each case. The slides were de-identified, randomized, and independently reviewed by 3 gastrointestinal pathologists. The diagnosis of dysplasia was established by the 5th edition of WHO for biliary intraepithelial neoplasia (BilIN). Consensus among three gastrointestinal pathologists was achieved before inclusion into the study (2 cases excluded due to lack of consensus). As reactive atypia, dysplasia and carcinoma is often focal, IMP3 immunohistochemical analysis was performed in corresponding areas with appropriate histological changes and graded as ++(> 80% cells +), + (5-80% cells +), and - (< 5% cells +). Chi-square test is used for statistical analysis.

Results: Of the 67 selected cases, 78% patients were white Hispanic, 21% non-Hispanic (14% white; 5% Black; 2% Pacific islander); 20% male and 80% female; age 19 to 87 years old (average 44). Clinical indications for cholecystectomy included acute and chronic cholecystitis, cholelithiasis and gallbladder polyp/mass. IMP3 expression is shown in Table 1. IMP expression is significantly higher in high-grade/invasive carcinoma (combined) than in reactive atypia (p=0.002) (Figure 1). There is no significant difference in IMP3 expression between reactive atypia and low-grade dysplasia (p=0.09) and between low-grade and high-grade dysplasia (p=0.28).

IMP3	NL	RA	LGD	HGD	IAC
	n(%)	n(%)	n(%)	n(%)	n(%)
-	2(100%)	18(52.9%)	5 (23.8%)	0(0%)	1 (14.3%)
+	0(0%)	11(32.4%)	11(52.4%)	1 (33.3%)	1(14.3%)
++	0 (0%)	5 (14.7%)	5 (23.8%)	2(66.7%)	5 (71.4%)

NL: Normal mucosa; RA: Reactive atypia; LGD: Low-grade dysplasia; HGD: High-grade dysplasia; IAC: Invasive adenocarcinoma

Figure 1 - 1143

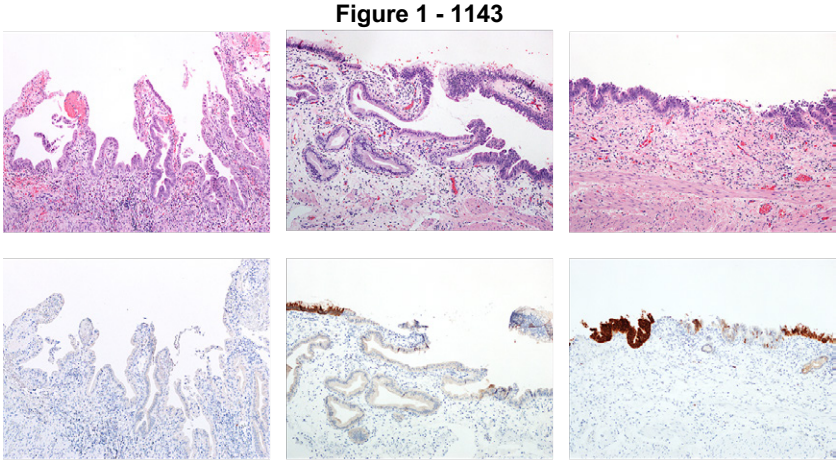

RA LGD HGD

Conclusions: The role of IMP3 expression in differentiating reactive atypia, low-grade and high-grade dysplasia of gallbladder mucosa is limited and should be interpretated with caution in the appropriate morphologic setting.

1144 Molecular Analysis Reveals Novel Somatic Alterations in Resected Gallbladder Carcinomas

Zhen Zhao[1], Stephen Ward[1]
[1]*Icahn School of Medicine at Mount Sinai, New York, NY*

Disclosures: Zhen Zhao: None; Stephen Ward: None

Background: Gallbladder cancer (GBC) often presents at an advanced stage and has a dismal prognosis. Molecular characterization of GBC has thus far been limited. Our institution utilizes the SEMA4 solid tumor panel, a next generation sequencing analysis of 161 of the most relevant cancer drivers. We report several novel molecular alterations in GBC from our institution identified by the SEMA4 panel.

Design: SEMA4 solid tumor panel was applied to 10 cases of surgically resected GBC. Demographics, tumor size, grade, stage, and histologic subtype were recorded. Molecular findings were compared with existing published data.

Results: We identified 10 patients with GBC that underwent molecular analysis by SEMA4 (5 male, 5 female, median age 68 years). Mean tumor size was 2.2 cm, 2 were well-, 6 were moderately-, and 2 were poorly-differentiated while 2 were pT1, 6 were pT2 and 2 were pT3. The histologic subtype was not otherwise specified in 8 and mucinous in 1, while 1 had signet ring cell features. Overall, 42 somatic genetic alterations involving 34 genes were identified. Of these, 28 variants in 22 genes were Tier 1 or Tier 2 changes with strong or potential clinical significance of therapeutic, prognostic and diagnostic actionability, while 14 were Tier 3, yet observed at a significant allele frequency in the general or specific databases. The average detected alteration number/patient was 4.4 (3.0 Tier 1/2, 1.4 Tier 3; overall range 1-11).

TP53 mutation was seen in 7 cases (6 different variants), MDM2 amplification in 2, and ARID1A SNVs in 2, similar to published frequencies, though 4 of the 6 TP53 variants have not been previously reported in GBC. All other alterations were seen in 1 patient each. We found alterations in RHOA and CDK2, previously not reported in GBC. Novel Tier 1/2 alterations were seen in ATR, BAP1, NOTCH1, SETD2, CTNNB1, PIK3R1, PIK3CA and EGFR, and novel Tier 3 variants of ARID1A, ATXR, CHEK1, RAD51C, FANCA, NOTCH 3, SETD2, SMARCB1, PIK3CB, NF1, and ESR1 were identified. Using Cytoscape, an open-source bioinformatics platform for visualizing molecular interaction networks, preliminary analysis highlights activation of ERBB, PI3K and Ras signaling, non-RTK signaling, and impaired DNA damage response.

Conclusions: Our work highlights several new genetic alterations that may be important in the pathogenesis of GBC. Validation of these findings may lead to potential targeted therapies and improved patient outcomes for these devastating tumors.